minerals

MDPI

Article

Insights into Elemental Migration-Enrichment Patterns and Microbial Communities in Tea Rhizosphere Soils Under Contrasting Lithological Backgrounds

Ruyan Li [1], He Chang [1,*], Ping Pan [2], Lili Zhao [3], Yinxian Song [1,*], Yunhua Hou [4], Haowei Bian [1], Jiayi Gan [1], Shuai Li [1], Jibang Chen [1], Mengli Xie [1], Kun Long [1], Wei Zhang [1] and Weikang Yang [1]

1 Faculty of Land Resources Engineering, Kunming University of Science and Technology, Kunming 650093, China; liruyan@stu.kust.edu.cn (R.L.)
2 Geomatics Engineering Faculty, Kunming Metallurgy University, Kunming 650033, China
3 College of Economics and Management, Pu'er University, Pu'er 665000, China
4 Kunming Comprehensive Survey Center for Natural Resources, China Geological Survey, Kunming 650111, China
* Correspondence: hechang@kust.edu.cn (H.C.); songyinxian@gmail.com (Y.S.)

Abstract

Elemental migration and enrichment are important processes influencing tea plant growth and the assembly of rhizosphere bacterial communities within the rock–soil–plant continuum. This study explores how soil parent materials (granite, quartz schist, and sericite schist) are potentially associated with these processes and their observed associations with the elemental composition of tea leaves. Exploratory statistical analyses revealed distinct, lithology-specific biogeochemical patterns that serve as a foundation for hypothesis generation. In granite soils, chlorite correlated with the mobility of Cr, Pb, Cu, Ni, Mg, and Na, coinciding with shifts in the relative abundances of Verrucomicrobia, Armatimonadetes, and Chloroflexi. In quartz schist, kaolinite exhibited notable correlations with the dynamics of Pb, Cr, Ni, Zn, and As, which were statistically linked to Planctomycetes, Proteobacteria, and Acidobacteria. Complex mineral–microbe interactions were observed in sericite schist soils, where clay minerals (e.g., chlorite, illite) were closely associated with the migration of multiple elements (Pb, K, Ca, Cd, As, Al, Fe, Zn), paralleling structural variations in communities of Actinobacteria, Planctomycetes, Chloroflexi, and Proteobacteria. Potassium (K), calcium (Ca), and manganese (Mn) showed bioaccumulation tendencies in tea leaves across all lithologies, with an enrichment capacity order of Ca > K > Mn > Mg > Na > Al. Exploratory Classification and Regression Tree (CART) analysis suggested that the migration of K, Ca, Cu, Zn, and Hg corresponded most closely with their soil concentrations. Manganese (Mn) exhibited a mineral-associated trend, with kaolinite content as a potential correlate, while cadmium (Cd) migration was statistically linked to the relative abundance of Armatimonadetes. These findings highlight potential candidate relationships between mineralogy, microbes, and elemental mobility rather than confirming causal mechanisms, emphasizing the need for further validation in larger or experimental datasets.

Keywords: Pu-erh tea plantations; bacterial community; trace element; migration; enrichment; rock–soil–plant continuum

Academic Editor: Rafael Santos

Received: 21 January 2026
Revised: 18 March 2026
Accepted: 19 March 2026
Published: 21 March 2026

1. Introduction

China is the birthplace of tea (*Camellia sinensis* L.), and historical records demonstrate that its tea-drinking culture has a long and continuous heritage spanning millennia [1].

The Yunnan–Guizhou Plateau in southwestern China is the cradle of tea plants. Yunnan's favorable natural environment and climate offer an exceptional foundation for the propagation and growth of Camellia sinensis, with abundant wild tea varieties of excellent quality and a long history of cultivated tea, making it a significant area for tea research [2]. Tea serves not only as an important cultural emblem but also as a health-promoting beverage rich in Ca and diverse bioactive compounds, with evidence indicating its efficacy in preventing cardiovascular and cerebrovascular diseases—further substantiating its positive impact on human health [3].Tea plants thrive in acidic soils, with an optimal cultivation pH range of 4.5–5.5, and soil pH is widely recognized as a primary factor associated with the enrichment of major elements, including Ca, Mg, Mn, and Al [4]. In acidic soils, tea plants exhibit increased accumulation of Mn [5]. Moreover, the quality of tea is closely linked to the chemical properties of the soil, and mineral concentrations in soil exhibit geographic variability [6]. Geographic location and soil type are recognized as important factors contributing to differences in soil nutrient and pH status across tea-growing regions [7].

Investigating the antagonistic stress effects arising from the migration and enrichment of major and trace elements through the rock–soil–tea continuum under different geological backgrounds is of significant importance for optimizing tea cultivation. Ca and Al exhibit a competitive relationship in the element absorption of tea plant roots [8]. Although tea plants tolerate toxic Al^{3+} due to their acidophilic nature, elevated Al concentrations disrupt the accumulation of essential nutrients—such as Ca, Mn, Mg, and Fe—in roots, leading to oxidative stress, cellular damage, and inhibited root growth [9].

In addition to studies on the mobility and accumulation of major elements such as Al, Mn, and K in tea plants, extensive research has also focused on the transfer and enrichment of trace elements. The primary sources of trace elements in tea garden soils include parent bedrock, geological processes, pesticides and fertilizers, atmospheric deposition, and weathering [10]. A range of geochemical factors—such as bedrock lithology, soil texture, and organic matter content—along with tea cultivar and fertilizer application, are considered potential determinants influencing the transfer of trace elements from soil to tea leaves [11,12]. Geological differences often play a significant role in influencing the distribution of trace elements—such as As, Zn, Cu, Cd, Pb, Hg, Cr, and Ni—in soils and their subsequent accumulation in tea leaves. Significant variations in trace element concentrations exist across different stratigraphic units and bedrock lithologies. Through rock weathering and pedogenesis, trace elements contained in the parent rock are released into the soil. Tea plant roots typically inhabit acidic soil environments, and acidification of tea plantation soils increases the concentrations of bioavailable trace elements—particularly their water-soluble and exchangeable forms—thereby enhancing their release and enrichment in the rhizosphere soil [13]. Most As in soils is primarily associated with organic matter and Fe–Mn oxides, and its concentrations vary significantly across different soil locations, depths, and fractions [14]. Trace elements are predominantly enriched in the roots, whereas elements such as Zn, Cu, and Ni—which are closely related to protein and enzyme synthesis in tea plants—are largely translocated to the stems and leaves [15]. During the life cycle of tea plants, trace elements can enter plant tissues through the roots, where they are absorbed via ion exchange, adsorption, and transport mechanisms, and subsequently accumulate in the leaves. Long-term accumulation of As, Cd, Pb, Cr, Mn, Ni, Cu, and Zn in human organs poses potential carcinogenic risks [16,17]. The distribution of elements in tea plants is not only regulated by the parent material but also influenced by antagonistic interactions. For example, phosphorus (P) and zinc (Zn) are both essential nutrients for tea growth; however, they can react in soils to form zinc phosphate [$Zn_3(PO_4)_2$] precipitates, thereby reducing the bioavailability of both elements. Moreover, excessive P concentrations in soils may inhibit Zn uptake by roots, leading to growth retardation in tea plants [18].

Research on soil nutrients and bacterial communities in tea plantations is of great significance for improving tea yield and enhancing soil health [19,20]. Current studies on the microbial composition of tea plantation soils mainly focus on the functional traits of bacterial communities and their associations with environmental drivers, tea plant health, and leaf quality [21,22]. Dominant bacterial phyla in tea plantation soils include Acidobacteria, Actinobacteria, Bacteroidetes, Chloroflexi, Planctomycetes, Proteobacteria, and Verrucomicrobia. The diversity of rhizosphere bacterial communities is closely linked to environmental factors [23,24]. Geographical heterogeneity, tea plantation types, cultivation practices, and tea tree varieties are considered major factors shaping the geochemical properties of soils and the composition of microbial communities in tea plantations [25–29]. In particular, spatial distance effects are strongly associated with bacterial community structure as well as functional variation in processes such as nitrification and nitrogen fixation [30], and the bacterial taxa enriched in rhizosphere surface soil, rhizosphere soil, and root endorhizosphere differ markedly [31]. Moreover, soil microorganisms further promote nutrient cycling, while nutrient availability reciprocally shapes microbial survival and activity. For example, magnesium enhances the relative abundance of beneficial taxa such as nitrogen-fixing bacteria and phosphate-solubilizing bacteria (PSB) [32,33]. Soil pH, exchangeable Mg^{2+}, and Ca^{2+} are generally positively correlated with bacterial diversity, and they may act as significant environmental drivers of bacterial community structure. These environmental factors, together with microbial communities, are thought to participate in regulating the distribution of N, K, Ca, Al, and Mg in tea leaves [34]. Given the acidic nature of tea garden soils, increasing soil acidification further reduces potassium availability, leaving much of the soil K inaccessible to plants. Under these conditions, potassium-solubilizing bacteria (KSB) facilitate plant uptake by releasing organic acids and chelators that dissolve K-bearing minerals such as orthoclase and mica, converting insoluble K into plant-available forms [35–37].

Microbe–mineral interactions modulate nutrient cycling by mediating mineral weathering processes. Minerals provide both energy and nutrient sources for microbial growth, while microbial metabolic activities regulate mineral dissolution, transformation, and precipitation, thereby initiating gene-controlled or metabolism-induced biomineralization processes [38,39]. Trace elements not only interfere with the uptake and distribution of essential major elements in tea plants, often leading to ionic substitution that results in nutrient deficiency and imbalance in soils, but also suppress soil microbial enzyme activities and disrupt nucleic acid structures [40]. Concurrently, trace element stress exerts potential impacts on the composition, functional abundance, and diversity of microbial communities in tea garden soils [41], with Cd, Hg, and Cu suggested as factors associated with bacterial community structures [42]. Soil bacteria possess diverse trace element resistance mechanisms [43].For example, Acidobacteria can regulate Fe–N coupled cycling and cation competition to suppress Cd transport and accumulation in plant roots [44]. Certain bacterial taxa employ specialized detoxification mechanisms to tolerate trace element stress (e.g., Hg, Pb, Cd, As) [45]. Concurrently, microbial metabolic activities actively modulate elemental speciation in soils. For instance, specific Pseudomonas and iron-oxidizing bacteria secrete multicopper oxidases that catalyze the oxidation of soluble Mn(II) into insoluble Mn(IV) oxides [46]. Although this biogenic precipitation reduces direct Mn bioavailability, it plays a crucial role in rhizosphere detoxification; the highly reactive Mn(IV) oxides effectively sequester toxic trace elements, thereby potentially enhancing plant resilience against environmental stressors [47]. In soils supplemented with Fe and Zn, microbial diversity was significantly reduced [48]. Under the mediation of soil organic matter, trace elements (e.g., Zn, Pb, Cu, Cr, As) further shape the structure of soil microbial communities [49]. In turn, microbial community composition and biochemical activities strongly influence rock

https://doi.org/10.3390/min16030333

weathering and soil formation processes, feeding back into plant growth by regulating the release and cycling of major elements in soils [50].

A large body of research has focused on trace elements, tea consumption risk assessments, and the structural characteristics of soil microbial communities. However, studies examining the similarities and differences in soil bacterial composition across tea gardens with varying geological and lithological backgrounds, as well as the potential influencing factors, remain limited. Moreover, the microbial responses and driving factors influencing community dynamics during elemental migration and accumulation are still poorly understood. Based on the fundamental role of parent materials, we hypothesize that: (1) distinct bedrock lithologies may create unique soil geochemical profiles, selectively enriching specific major and trace elements; and (2) these lithology-driven variations—particularly trace element stress—could potentially alter the diversity, assembly, and adaptive responses of soil bacterial communities. Therefore, in this study, we collected bedrock, soil, and tea leaf samples from 13 representative tea gardens in Yunnan Province with different lithological backgrounds to conduct an exploratory analysis of their elemental composition and the functional structure of soil bacterial communities. Given the localized scale of this dataset, our analyses are intended to organize patterns and generate hypotheses rather than confirm definitive mechanisms. We aimed to explore: (a) the potential differences in soil bacterial community structure and diversity under distinct lithological backgrounds; (b) the candidate factors associated with root-associated bacterial responses and microbial community shifts under trace element stress; and (c) the preliminary associations between soil microbial communities and elemental migration and accumulation within the rock–soil–tea ecosystem under different lithological conditions.

2. Materials and Methods

2.1. Study Area

The study area is located in the tea-producing regions of Shuangjiang and Yunxian, Lincang City, Yunnan Province, China (23°47′42″–24°32′38″ N, 99°85′68″–100°16′61″ E), which is recognized as the native habitat of the world-renowned Yunnan large-leaf tea variety (*C. sinensis var. assamica cv. Yunnan-daye*). Situated on the Yunnan–Guizhou Plateau, the area has a subtropical low-latitude monsoon climate, with elevations ranging from 1400 to 2500 m, a mean annual temperature of 17.3 °C, and annual precipitation of 920–1750 mm. The exposed strata are mainly from the Permian of the Paleozoic to the Upper Tertiary of the Cenozoic, with lithologies dominated by quartz schist, granite, and sericite schist. The prevailing soil types are brown earth and yellow-brown earth (Figure 1).

2.2. Sampling and Analytical Methods

2.2.1. Sampling Design

Based on lithological variations, 13 representative Pu-erh tea plantations were selected to investigate the biogeochemical patterns of rock, soil, and tea leaf samples across the study area. To ensure appropriate structuring of this localized dataset, these 13 plantations were categorized into three groups according to their underlying parent bedrock, serving as exploratory replicates for identifying lithology-specific patterns: granite (GT, n = 5), quartz schist (QS, n = 4), and sericite schist (SS, n = 4) (Table 1). Fresh tea leaves were sampled in each plantation using the five-point sampling method around a single tree, and subsequently pooled into a composite sample. Rhizosphere soil samples were collected from the same sites using the five-point sampling method by removing surface debris and sampling at a depth of 5–15 cm, which were homogenized into a composite sample. In parallel, rhizosphere soil was collected under sterile conditions for microbial analysis. Prior to sampling, all tools were sterilized with anhydrous ethanol. Soil samples for microbial analysis were immediately transferred to sterile centrifuge tubes, stored at −80 °C, and later processed under low-temperature conditions in the laboratory for DNA extraction and sequencing.

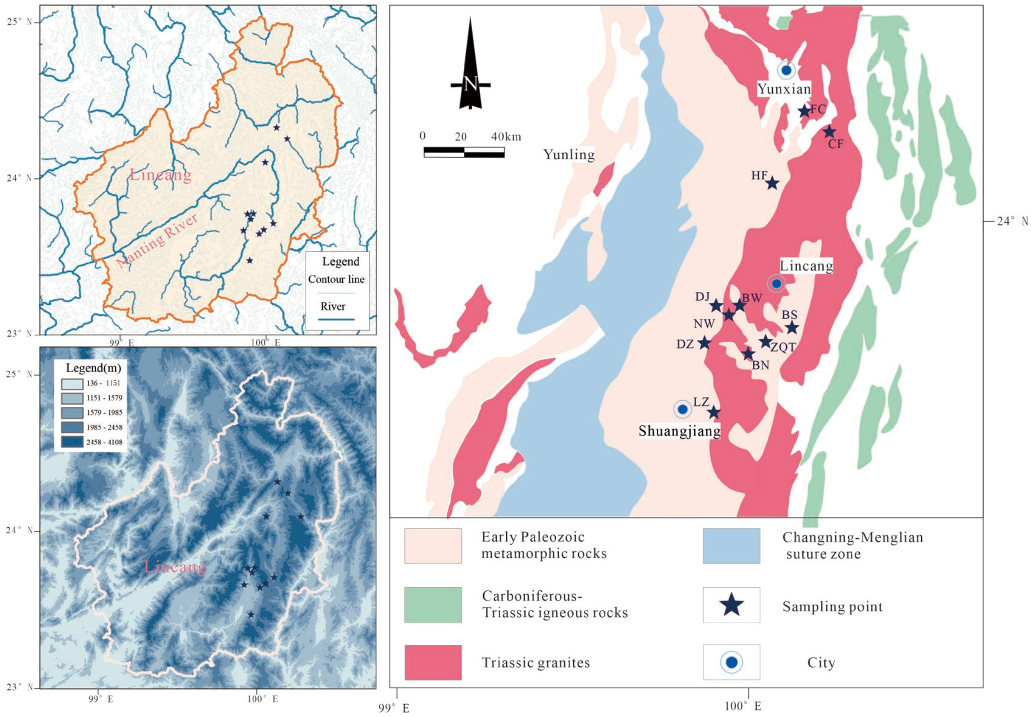

Figure 1. Simplified geologic map of the Lincang area showing major geologic units.

Table 1. Sampling Table: Rock, Soil, Tea Leaf, and Microbial Samples. Unit: pieces.

Lithology	Rock	Soil	Soil Microbial	Tea
Granite	R-GT1 R-GT2 R-GT3 R-GT4 R-GT5	S-GT1 S-GT2 S-GT3 S-GT4 S-GT5	B-GT1 B-GT2 B-GT3 B-GT4 B-GT5	T-GT1 T-GT2 T-GT3 T-GT4 T-GT5
Quartz schist	R-QS1 R-QS2 R-QS3 R-QS4	S-QS1 S-QS2 S-QS3 S-QS4	B-QS1 B-QS2 B-QS3 B-QS4	T-QS1 T-QS2 T-QS3 T-QS4
Sericite schist	R-SS1 R-SS2 R-SS3 R-SS4	S-SS1 S-SS2 S-SS3 S-SS4	B-SS1 B-SS2 B-SS3 B-SS4	T-SS1 T-SS2 T-SS3 T-SS4

2.2.2. Geochemical Analyses

Fresh tea leaves were weighed, oven-dried at 80 °C to constant weight, and ashed in a muffle furnace at 450 °C for 2 h. The resulting powder was used for elemental analysis. Approximately 0.2–0.5 g of powdered sample was digested in a mixture of hydrochloric acid (HCl) (ρ = 1.19 g/mL), nitric acid (HNO_3) (ρ = 1.42 g/mL), and perchloric acid ($HClO_4$) (ρ = 1.68 g/mL) using a microwave digestion system at 120 °C under high pressure for 5 h. The digested solutions were diluted to 10 mL prior to elemental determination. Soil samples were air-dried, homogenized, and passed through a 200-mesh sieve for geochemical analyses, including pH, soil organic matter (SOM), elemental concentrations, and mineral composition. Soil pH was measured by a WTW pH530 meter with a soil-to-water ratio of 1:2.5. SOM content was measured by the potassium dichromate oxidation-external heating method. For rock and soil elemental analysis, ~0.2 g of finely ground sample was digested in a mixture of 5 mL HNO_3, 2 mL HF, 1 mL H_2SO_4, and 5 mL aqua regia in a microwave digestion system, cooled, and diluted to a constant volume. Tea leaf samples were quality-controlled using the biological standard reference material GBW10016 (GSB-7) [51], while soil samples were quality-controlled with GBW07385 (GSS-29) [52]. Chemical element concentrations were determined by inductively coupled plasma atomic emission spectrometry (ICP-AES; Prodigy, Teledyne Leeman Labs, Hudson, NH, USA). In accordance with ecological and geochemical assessment protocols, key elements were systematically analyzed, with relative standard deviations (RSD) of replicate measurements maintained below 5%. All chemical analyses were conducted under strict quality assurance and quality control (QA/QC) procedures to ensure analytical reliability and accuracy. Mineralogical compositions of soil and rock samples were identified using X-ray diffraction (XRD; BTX-526, Olympus, Center Valley, PA, USA).

2.2.3. Bioinformatic Processing

Soil microbial community composition was analyzed by 16S rRNA gene amplicon sequencing conducted by Shanghai GeneCowin Biotechnology Co., Ltd., Shanghai, China. Total genomic DNA was extracted using the FastDNA SPIN Kit for Soil (MP Biomedicals, Santa Ana, CA, USA). DNA integrity was verified by agarose gel electrophoresis, and concentration and purity were measured with a NanoDrop 2000 spectrophotometer (Thermo Fisher Scientific, Waltham, MA, USA). The V4–V5 hypervariable region of the 16S rRNA gene was amplified using the primers 515F (5′-GTGCCAGCMGCCGCGG-3′) and 907R (5′-CCGTCAATTCMTTTRAGTTT-3′), and sequenced on an Illumina NovaSeq 6000 platform with an SP-Xp (PE250) paired-end sequencing strategy. Raw sequencing data were processed and quality-controlled on the QIIME2 platform. Adapter sequences and primers were removed using the cutadapt plugin, followed by an assessment of raw data quality. High-quality sequences were obtained with the DADA2 plugin through filtering, denoising, merging, and chimera removal, thereby enhancing the accuracy of subsequent bioinformatic analyses, and generated feature tables and representative sequences. Representative Amplicon Sequence Variant (ASV) sequences were compared against reference databases to assign taxonomic annotations, with confidence thresholds set at 0.8 for 16S and 18S rRNA gene data, and 0.6 for ITS region data.

2.3. Weathering Indices and Enrichment Factors

A suite of geochemical indices was applied to evaluate the intensity of chemical weathering and the relative enrichment of elements in soils derived from different lithologies. These indices include the Chemical Index of Alteration(CIA), the Chemical Index of Weathering (CIW), the Weathering Index of Parker (WIP) [53–55], and enrichment-based parameters such as the Enrichment Factor and the Bioconcentration Factor (BCF) [56,57].

1. Chemical Index of Alteration (CIA)

The CIA is a widely used geochemical proxy for assessing the intensity of rock weathering, based on variations in the concentrations of major elements. It is defined as:

$$CIA = 100 \times Al_2O_3 / (Al_2O_3 + CaO^* + Na_2O + K_2O) \quad (1)$$

where CaO* represents the molar proportion of CaO derived exclusively from silicate minerals. Following the correction method of McLennan, the influence of non-silicate Ca is assessed using the molar ratio of CaO/Na_2O. If the ratio exceeds 1, the CaO content is replaced by that of Na_2O; otherwise, the measured CaO content is used to calculate CIA [58].

In general, CIA values between 50–65 indicate weak weathering, values between 65–80 represent moderate weathering, and values between 85–100 reflect intense weathering.

2. Chemical Index of Weathering (CIW)

The CIW, which excludes the effect of potassium variation relative to CIA, provides a more accurate measure of the loss of highly mobile elements such as Na and Ca. It is defined as:

$$CIW = 100 \times Al_2O_3 / (Al_2O_3 + Na_2O_2 + CaO) \quad (2)$$

Higher CIW values correspond to stronger chemical weathering. This index is particularly useful in systems where K-metasomatism may obscure weathering trends.

3. Weathering Index of Parker (WIP)

The WIP is a geochemical index used to quantify the extent of chemical weathering in silicate rocks and soils. It calculates the proportion of mobile alkali and alkaline earth metals (Na, K, Mg, Ca) remaining in the sample to gauge the intensity of weathering processes:

$$WIP = 100 \times (2 Na_2O/0.35 + MgO/0.9 + 2K_2O/0.25 + CaO^{*}/0.7 \quad (3)$$

Crucially, unlike the CIA and CIW, a lower WIP value indicates a higher degree of weathering, as intense weathering preferentially depletes these mobile cations from the soil profile.

4. Enrichment Factor (EF)

The EF is commonly applied to evaluate the extent of elemental migration and accumulation from parent rock to soil. Al, owing to its relative geochemical immobility and stability during weathering, is frequently employed as the reference element in EF calculations.

$$EF_i = (C_i/C_{Al})_{Soil} / (C_i/C_{Al})_{Rock} \quad (4)$$

where C_i represents the concentration of the selected element, and C_{Al} denotes the concentration of Al in the soil and underlying parent rock, respectively. An EF value greater than 1 indicates relative enrichment, whereas a value less than 1 indicates relative depletion.

5. Bioconcentration Factor (BCF)

The BCF is an important index for evaluating the transfer and accumulation potential of pollutants or beneficial elements from the environment into organisms. In plant–soil systems, it is defined as the ratio of the concentration of a given element in plant tissues (e.g., tea leaves) to its concentration in the corresponding soil, providing a direct measure of the accumulation tendency of chemical elements within the organism.

$$BCF = C_{Tea} / C_{Soil} \quad (5)$$

where C_{Tea} represents the concentration of the element in tea leaves, and C_{Soil} represents its concentration in soil. Higher BCF values indicate a greater potential for elemental accumulation, suggesting that the element is more likely to be absorbed and retained by the plant. Since the recognized Al-hyperaccumulating nature of tea plants renders Al non-conservative and unsuitable for normalization, the traditional Bioconcentration Factor (BCF) remains the most objective metric for evaluating elemental uptake in this study to avoid artificially depressing the enrichment indices of other elements.

2.4. Data Processing and Analysis

Bar plots of microbial community composition and relative abundance were generated in R (v3.3.0) using the ggplot2 package. α-diversity indices (Chao1, Shannon, and Simpson) were calculated with the vegan package(version 2.6-4). To examine potential lithological influences on β-diversity, bacterial principal coordinate analysis (PCoA) based on the Bray–Curtis distance matrix was performed using the ChiPlot platform (https://www.chiplot.online/). To identify emerging structural patterns, exploratory co-occurrence networks were visualized in Cytoscape (v3.10.3). One-way analysis of variance (ANOVA) followed by the Waller–Duncan post hoc test was performed in SPSS (v27.0). To highlight candidate environmental predictors of elemental migration, exploratory classification and regression tree (CART) models were developed. As detailed in the Supplementary Material, given the limited sample size, these CART models were utilized strictly as hypothesis-generating tools rather than for robust predictive modeling. Correlation heatmaps linking environmental variables to bacterial communities were produced in Origin (2021). Exploratory redundancy analysis (RDA) was performed and visualized in Canoco (v5.0) to highlight candidate associations between environmental factors and microbial structures.

3. Results

3.1. Geochemical Characteristics of Rock and Soil Elements in Tea Plantations with Different Lithologies

The elemental distribution of rock samples from the study area is summarized in Table 2. Concentrations of K, Mn, and Ca were highest in quartz schist, with K and Mn being lowest in granite and Ca being lowest in sericite schist, suggesting that elemental distribution is associated with mineralogical composition [59]. Na and Al were most abundant in granite and least abundant in sericite schist; the high Al content in granite is likely linked to magmatic differentiation processes [60]. Mg and Fe were most enriched in sericite schist. For trace elements, As, Hg, Ni, Cu, Zn, Cd, and Cr were most abundant in quartz schist, whereas Ni, Zn, Cd, and Cr showed the lowest concentrations in granite. Inclusions of Cr, Ni, Cu, and Zn were identified in sericite schist and quartz schist, occurring either in native forms or as oxides, sulfides, sulfates, phosphates, or intermetallic compounds [61]. Pb was highest in granite but lowest in sericite schist, reflecting potential crustal differentiation and evolutionary processes [62].

Soil samples exhibited pH values ranging from 4.67–6.34, all weakly acidic and consistent with the pH range favorable for tea growth. The mean soil pH was highest in quartz schist areas (5.57) and lowest in sericite schist areas (4.975). Soil organic matter (SOM) contents exceeded 36% across all samples, relatively high compared to soils under similar vegetation types [63]. SOM influences soil physicochemical properties, thereby potentially mediating the transformation and distribution of both major elements and trace elements [64]. Weathering enhances the oxidation and decomposition of SOM [65], and the sensitivity of SOM decomposition differs substantially across vegetation types [66].

The study area is located within the Lancang River fault zone, characterized by complex lithological assemblages and intense weathering. Weathering indices indicated that soils derived from all three lithologies are strongly weathered (CIA > 85). Such highly weathered soils are typically acidic [67], with quartz schist soils showing the highest degree of weathering and granite soils the lowest. Among major elements, K and Na were most enriched in granite soils, a pattern associated with weathering and mineral decomposition. Feldspars in granite release K and Na during advanced weathering, and granite soils are rich in orthoclase and plagioclase, both of which contain high concentrations of these elements [68,69]. Weathering also leads to the degradation of primary minerals into clay minerals, while alkaline earth metals and their cations are leached, resulting in low concentrations of Ca and Mg in surface soils [70].

Table 2. Soil properties and rock element content in tea plantations under different lithological conditions.

Group		GT	QS	SS	F	*p*
rock	K	2.312 ± 0.367 [a]	2.75 ± 0.479 [a]	2.459 ± 0.226 [a]	0.357	0.450
	Ca	0.247 ± 0.106 [a]	0.346 ± 0.272 [a]	0.21 ± 0.13 [a]	0.152	0.611
	Fe	3.584 ± 0.642 [a]	4.837 ± 0.438 [a]	4.939 ± 0.438 [a]	2.046	0.125
	Mg	1.108 ± 0.266 [a]	0.83 ± 0.216 [a]	1.299 ± 0.301 [a]	0.727	0.264
	Na	1.896 ± 0.472 [a]	0.409 ± 0.313 [b]	0.719 ± 0.319 [ab]	4.132	0.049
	Al	7.975 ± 0.389 [a]	7.166 ± 0.618 [a]	7.575 ± 0.217 [a]	0.891	0.240
	Mn	0.026 ± 0.006 [a]	0.068 ± 0.022 [a]	0.056 ± 0.005 [a]	2.920	0.055
	As	34.358 ± 12.735 [a]	91.304 ± 55.543 [a]	28.17 ± 8.407 [a]	1.211	0.199
	Hg	0.014 ± 0.004 [a]	0.032 ± 0.022 [a]	0.012 ± 0.003 [a]	0.789	0.300
	Ni	24.501 ± 5.643 [b]	41.554 ± 5.076 [a]	35.678 ± 1.478 [ab]	3.508	0.070
	Cu	191.182 ± 53.746 [a]	237.47 ± 91.107 [a]	161.288 ± 75.038 [a]	0.263	0.494
	Zn	45.29 ± 10.959 [a]	86.055 ± 21.976 [a]	73.738 ± 3.772 [a]	2.383	0.077
	Cd	0.183 ± 0.047 [a]	0.237 ± 0.077 [a]	0.191 ± 0.076 [a]	0.200	0.587
	Pb	12.513 ± 4.139 [a]	10.178 ± 1.37 [a]	7.812 ± 3.593 [a]	0.474	0.384
	Cr	75.136 ± 25.332 [a]	129.67 ± 25.998 [a]	83.74 ± 6.723 [a]	1.695	0.131
soil	PH	5.304 ± 0.242 [a]	5.57 ± 0.294 [a]	4.975 ± 0.124 [a]	1.486	0.120
	SOM	5.08 ± 13.683 [a]	5.18 ± 6.87 [a]	3.67 ± 4.28 [a]	0.651	0.344
	K	2.148 ± 0.373 [a]	1.485 ± 0.097 [a]	1.693 ± 0.398 [a]	1.092	0.211
	Ca	0.153 ± 0.069 [a]	0.1 ± 0.028 [a]	0.075 ± 0.019 [a]	0.652	0.325
	Fe	4.284 ± 0.206 [a]	5.453 ± 0.744 [a]	4.068 ± 0.218 [a]	2.809	0.056
	Mg	0.818 ± 0.183 [a]	0.565 ± 0.08 [a]	0.395 ± 0.046 [a]	2.662	0.058
	Na	0.141 ± 0.055 [a]	0.105 ± 0.036 [a]	0.056 ± 0.02 [a]	1.011	0.212
	Al	8.664 ± 0.529 [a]	9.233 ± 0.227 [a]	8.398 ± 0.684 [a]	0.619	0.308
	Mn	0.052 ± 0.015 [ab]	0.108 ± 0.035 [a]	0.031 ± 0.007 [b]	3.124	0.088
	As	9.924 ± 2.07 [a]	35.69 ± 18.675 [a]	72.635 ± 37.65 [a]	2.056	0.086
	Hg	0.076 ± 0.02 [ab]	0.105 ± 0.016 [a]	0.041 ± 0.006 [b]	3.484	0.071
	Ni	32.58 ± 2.661 [b]	43.7 ± 4.08 [a]	26.7 ± 1.967 [b]	7.724	0.009
	Cu	26.72 ± 5.242 [a]	39.175 ± 7.737 [a]	21.5 ± 2.012 [a]	2.526	0.056
	Zn	76.98 ± 7.402 [a]	85.275 ± 12.995 [a]	55.925 ± 6.347 [a]	2.563	0.056
	Cd	0.106 ± 0.024 [a]	0.093 ± 0.037 [a]	0.053 ± 0.009 [a]	1.144	0.196
	Pb	29.08 ± 2.708 [a]	34.9 ± 8.264 [a]	25.5 ± 1.424 [a]	0.911	0.216
	Cr	97.7 ± 14.424 [a]	129.83 ± 16.501 [a]	92.45 ± 13.766 [a]	1.726	0.124
	CIA	84.842 ± 2.55 [a]	89.395 ± 0.595 [a]	87.912 ± 1.941 [a]	1.367	0.164
	WIP	2359.697 ± 424.41 [a]	1635.93 ± 91.88 [a]	1761.55 ± 400.39 [a]	1.222	0.207
	CIW	97.524 ± 1.038 [a]	98.451 ± 0.461 [a]	98.847 ± 0.158 [a]	0.862	0.264

Values are presented as mean ± standard deviation (n = 4–5). Significant differences ($p < 0.05$) were determined by one-way ANOVA followed by an LSD test. Different lowercase letters within the same row indicate significant differences. The unit for SOM, K, Ca, Mg, Fe, Al, Na, and Mn is %; and for Cu, Zn, Cr, Pb, Cd, Hg, Ni, and As is $mg \cdot kg^{-1}$.

Mn, an important redox catalyst, potentially influences trace element concentrations and distributions in soils. Mn oxides may promote the biogeochemical cycling of various trace elements, and the bioavailability of Mn has been associated with soil bacterial community structure [71]. The relatively low Mn content in sericite schist soils could be attributed to the influence of soil pH on element solubility and availability, as Mn supply depends not only on soil chemistry but also on plant metabolism and microbial activity [72]. All soils exhibited relatively high Al contents, likely due to the weathering of silicate-rich minerals in parent rocks. For trace elements, Cr was relatively enriched and Hg depleted in granite and quartz schist soils, potentially because under weakly acidic conditions, organic matter-rich soils more strongly adsorb Cr but weakly absorb Hg. Moreover, complex stratigraphy may inhibit Hg adsorption by clay minerals [73]. Arsenic (As) in soils occurs predominantly in inorganic forms [74]. Geological processes such as volcanism and sedimentation release As from the crust, which subsequently accumulates during diagenesis [75]. Soil microorganisms further modulate As bioavailability and mobility, reducing its environmental risk [76].

Compared with crustal averages, Ca, Na, and Hg concentrations were below average in soils, whereas Cu and As were substantially higher [77].

In comparison, although Mg abundance in parent rocks was higher in sericite schist than in granite, this trend reversed in the soils, where Mg concentrations were higher in granite soils than in sericite schist soils. This may be explained by the dissolution of silicate minerals and the formation of Mg-adsorbing clay minerals during granite weathering [78]. The depletion of major elements in soils relative to their parent rocks suggests elemental losses during weathering, likely resulting from the dissolution of primary minerals, followed by leaching by groundwater or uptake by plants [79]. In contrast to their distribution in rocks, Fe, Pb, and Hg were relatively enriched in quartz schist soils, suggesting the release of trace elements from parent rocks during weathering and subsequent migration and accumulation in soils [80,81]. Overall, the geochemical characteristics of soils are shaped by multiple interacting factors. Parent material not only influences soil formation and development [82] but also imposes constraints on geochemical characteristics [83], which in turn show potential associations with bacterial community composition. Moreover, soil elemental distributions appear to be jointly influenced by geological background, anthropogenic activity, and pedogenic processes, with surface adsorption by clay minerals and SOM complexation-stabilization playing critical roles [84].

3.2. Mineralogical Characteristics of Rocks and Soils in Tea Plantations with Different Lithologies

The mineralogical composition of parent rocks varies significantly among different lithologies, which shows potential associations with the distribution of elements (Table 3). Granite is mainly composed of K-feldspar, plagioclase, and biotite, with feldspar contents markedly higher than those in the other two lithologies [85,86]. Granite also exhibits the highest Na and Pb concentrations (Table 2). This is likely associated with the abundance of K and Na in feldspars; during magmatic crystallization, Pb, with an ionic radius similar to that of K^+, readily substitutes for K^+ into the feldspar lattice, contributing to the observed enrichment [87,88]. In quartz schist, quartz, muscovite, and limonite are dominant. The mineralogical properties of quartz are influenced by its defect structures, which enable extensive isomorphous substitution, such as Al^{3+} and Fe^{3+} replacing Si^{4+} in the lattice [89,90]. Limonite, an essential constituent of quartz schist, is enriched in Fe, Mn, and Ni, and contains minor amounts of Cu and Zn [91–94], potentially explaining the elevated Mn, Ni, Cu, and Zn contents in quartz schist (Table 2). Sericite and chlorite predominantly occur in sericite schist. Previous studies have indicated that K, Ca, and Na contents in sericite schist are lower than in other lithologies [59]. Chlorite is dominated by Fe and Mg [95], consistent with the highest Fe and Mg concentrations observed in sericite schist (Table 2).

The distribution of secondary minerals in soils exhibits pronounced lithological differences. Soils derived from granite are enriched in plagioclase, illite, and K-feldspar, whereas quartz and chlorite dominate in quartz schist soils, and montmorillonite and kaolinite are abundant in sericite schist soils. Illite, a K-rich mineral [96], likely contributes to the highest K contents observed in granite soils (Table 2). Unlike primary minerals, secondary minerals may modulate element distribution through surface adsorption–desorption, dissolution–precipitation, and redox reactions. Illite and 2:1 layered clay minerals release fixed or non-exchangeable K via ion exchange, while montmorillonite retains Ca^{2+}, Mg^{2+}, K^+, and Na^+ in exchangeable form [97,98]. On the surface of kaolinite, Cu^{2+}, Zn^{2+}, and Ni^{2+} can form inner-sphere complexes, thereby potentially immobilizing trace elements. Moreover, montmorillonite and kaolinite are known to possess strong adsorption capacities for heavy metals and trace elements such as As, Cd, Cr, Fe, Pb, and Mn [99,100]. However, clay minerals can form inner- or outer-sphere complexes with soil organic matter (SOM), and

https://doi.org/10.3390/min16030333

such complex interfacial interactions could influence trace element binding behaviors [101], further affecting the immobilization of trace elements in soils.

Table 3. Mineral content of rocks and soils under different lithological backgrounds.

Group		GT	QS	SS	F	*p*
rock	Quartz	26.026 ± 4.762 [b]	63.048 ± 0.32 [a]	20.695 ± 3.109 [b]	38.196	0.000
	sericite	4.238 ± 1.545 [c]	28.29 ± 0.34 [b]	62.305 ± 2.195 [a]	273.983	0.000
	Plagioclase	37.862 ± 4.265 [a]	9.87 ± 5.5 [b]	13.397 ± 0.463 [b]	13.886	0.004
	K-feldspar	20.576 ± 2.801 [a]	-	1.07 ± 0 [b]	8.080	0.047
	Muscovite	8.43 ± 0 [a]	19.415 ± 9.265 [a]	-	0.469	0.618
	Limonite	3.124 ± 0.88 [a]	4.97 ± 0.51 [a]	2.558 ± 0.771 [a]	1.368	0.308
	Biotite	9.17 ± 1.344 [a]	7.705 ± 2.945 [a]	3.32 ± 0 [a]	1.410	0.344
	Chlorite	-	1.828 ± 0.912 [a]	4.397 ± 1.633 [a]	2.17643	0.20016
soil	Quartz	46.57 ± 2.65 [b]	71.498 ± 2.912 [a]	42.99 ± 0.872 [b]	39.310	0.000
	Plagioclase	7.866 ± 1.39 [a]	4.64 ± 0 [a]	2.255 ± 0.233 [a]	6.271	0.028
	Chlorite	4.67 ± 0.454 [b]	8.77 ± 0.711 [a]	3.23 ± 1.09 [b]	10.286	0.008
	Illite	17.738 ± 1.096 [a]	17.463 ± 2.385 [a]	17.46 ± 0.682 [a]	0.012	0.988
	K-feldspar	1.382 ± 0	-	-	-	-
	Montmorillonite	-	1.34 ± 0	3.54 ± 0	-	-
	Kaolinite	23.642 ± 1.222 [b]	2.968 ± 1.968 [c]	32.295 ± 1.036 [a]	102.671	0.000

Values are expressed as mean ± SD (n = 4–5). Different letters in the same row indicate significant differences ($p < 0.05$) by one-way ANOVA with an LSD test. Unit: %.

The mineralogical results of both rocks and soils suggest that mineral weathering is an important process mediating element cycling. Lithology appears to constrain the distribution of major elements and trace elements in soils. Within this dataset, distinct associations between trace elements and specific minerals are observed: Pb, Cd, Cu, and Zn are primarily associated with Al- and Fe-bearing minerals (e.g., micas), whereas Cr and Ni are primarily linked with Mg-bearing minerals (e.g., montmorillonite). The relative enrichment of trace elements in soils across the study area is likely associated with the high adsorption affinity of clays such as mica and montmorillonite [102]. In these systems, The transformation of clay minerals is accompanied by element migration. Feldspar and mica enriched in Ca^{2+} and Mg^{2+} undergo dissolution and K^+ release, leading to the formation of illite and kaolinite. Dissolution of Al^{3+}- and K^+-bearing feldspars and micas releases K^+, producing chlorite; removal of K^+ and Ca^{2+} yields kaolinite, while loss of Ca^{2+} and Na^+ results in montmorillonite. Kaolinite can transform into chlorite under Mg^{2+}- and Fe^{2+}-rich conditions, whereas montmorillonite may convert into illite in Al^{3+}- and K^+-rich environments [103,104]. The composition and structure of minerals not only potentially influence element release and fixation but also may affect bioavailability through interactions with organic matter [105]. Furthermore, minerals show preliminary associations with the structure and composition of soil bacterial communities, suggesting roles that may extend beyond merely serving as inert substrates [106,107].

3.3. Bacterial Community Structure in Tea Plant Rhizosphere Soils with Different Lithological

3.3.1. Bacterial Community Composition and α-Diversity

Rarefaction curves provided an exploratory indication of the adequacy of sequencing depth and the variation in species richness (Figure 2a). The results suggest that all sample curves plateaued as sequencing depth approached 10,000 reads, indicating that the sequencing depth was sufficient to represent the majority of bacterial taxa present in the samples. Alpha diversity indices, including Shannon and Simpson indices, reflect the richness and evenness of bacterial communities, while β-diversity—which assesses the dissimilarity in species composition between different communities—was used to characterize potential spatial shifts in microbial structure [107]. Analysis of α-diversity (Table 4) suggested differences between granite (GT) and quartz schist (QS) soils. Specifically, the Shannon index was higher in granite soils compared to quartz schist and sericite schist soils, suggesting a trend of greater bacterial community complexity in granite soils. By contrast, sericite schist and quartz schist soils displayed comparable α-diversity, with no significant differences detected. Soil bacterial community structure and diversity are potentially associated with factors such as parent material and geographic isolation, which may contribute to the distinct bacterial diversity patterns observed in tea plantation soils across different lithological backgrounds [108].

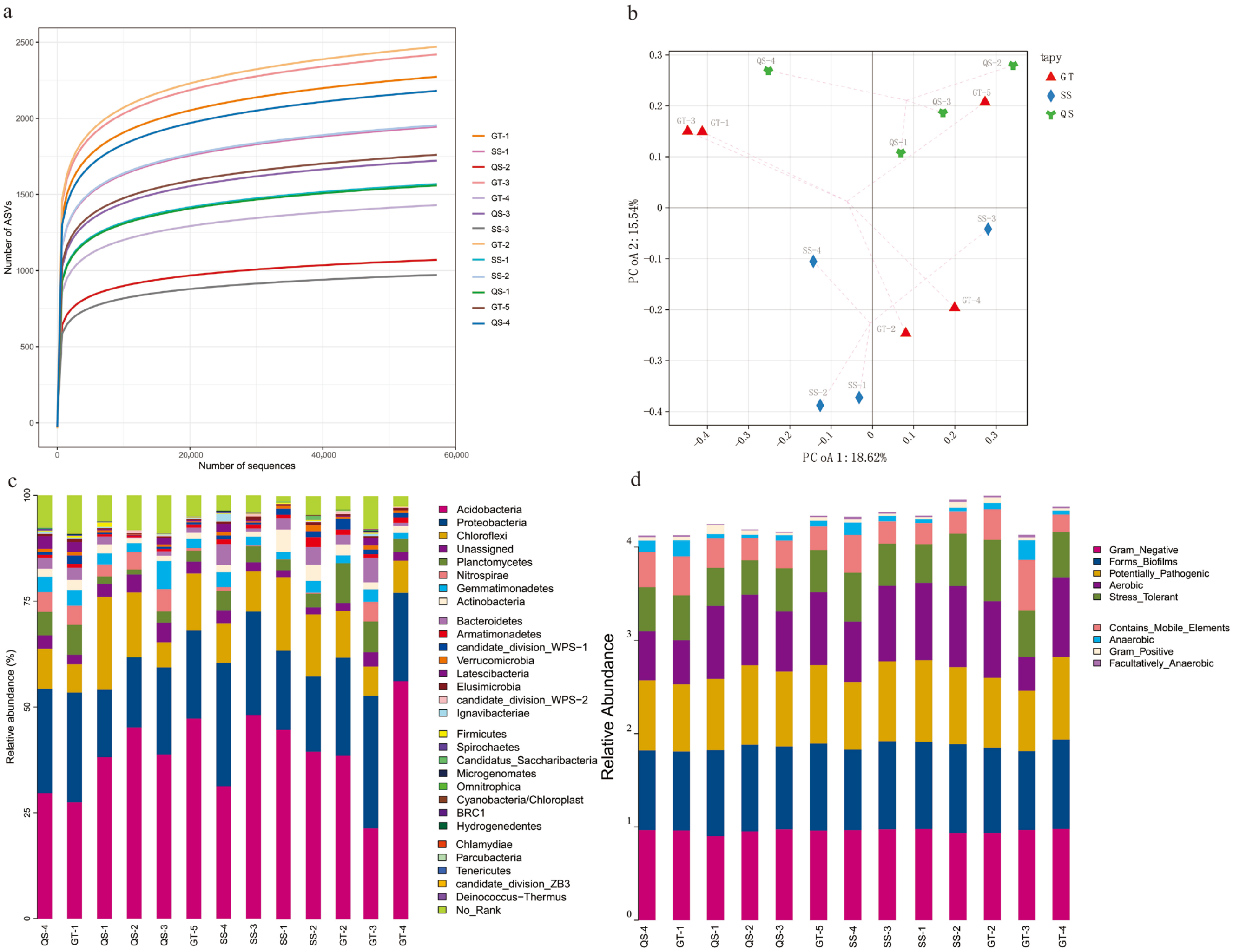

Figure 2. (**a**) Rarefaction curves of all samples from different sampling sites. The x-axis represents the number of sequences randomly selected from the samples, and the y-axis represents the number of observed Operational Taxonomic Units (OTUs). (**b**) Principal coordinates analysis (PCoA) plot. The x-axis (Axis.1) and y-axis (Axis.2) represent the two principal components that explain the greatest proportion of variation among samples. Closer distances between sample points indicate higher similarity. (**c**) Bacterial community composition at the phylum level. (**d**) Bacterial community composition based on functional classification. Each bar represents a group, with the y-axis showing the relative abundance. The sum of relative abundances for all species within a single group is 1.

Table 4. Alpha diversity indices of soil bacterial communities in each sample.

Group	GT	QS	SS	F	*p*
Observed	2059.6 ± 203.338 [a]	1627 ± 230.4 [a]	1780.75 ± 95.64 [a]	1.387	0.158
Chao1	2083.724 ± 208.22 [a]	1642.677 ± 229.746 [a]	1794.001 ± 95.624 [a]	1.418	0.155
ACE	2078.024 ± 205.323 [a]	1641.925 ± 231.736 [a]	1794.51 ± 95.738 [a]	1.392	0.158
Shannon	6.818 ± 0.178 [a]	6.324 ± 0.23 [a]	6.581 ± 0.093 [a]	1.984	0.091
Simpson	0.003 ± 0.001 [a]	0.005 ± 0.001 [a]	0.004 ± 0.001 [a]	2.326	0.071

Values are expressed as mean ± SD. Significant differences ($p < 0.05$) determined by one-way ANOVA with LSD test are indicated by different lowercase letters within the same column.

Bacterial β-diversity was explored using principal coordinate analysis (PCoA) based on the Bray–Curtis distance matrix ($p < 0.05$) (Figure 2b). Samples were evenly distributed across the four quadrants, with greater within-group dissimilarity observed among granite soils. This variability may be associated with differences in elemental composition and weathering intensity among the granite sampling sites [109]. By contrast, quartz schist and sericite schist samples clustered more closely, suggesting preliminary similarities in community structures within each lithology. However, the large separation between these two lithologies suggests that microbial community composition is associated with rock geochemistry within this limited dataset [110].

A total of 31 bacterial phyla were detected across all soil samples, with 11 phyla classified as dominant. The bacterial communities were primarily dominated by Acidobacteria, Proteobacteria, and Chloroflexi, together accounting for over 70% of the total abundance (Figure 2c). The potential for complex ecological relationships between various bacterial communities is highlighted [111]. Acidobacteria exhibited the highest relative abundance in sericite schist soils (40.92%) and the lowest in quartz schist soils (37.94%). 16S rRNA gene amplicon sequencing suggested that Acidobacteria distribution was relatively uniform in sericite schist and quartz schist soils but fluctuated widely across granite soils, paralleling the PCoA results (Figure 2b). Acidobacteria are widely distributed in terrestrial ecosystems, especially in acidic soils, where they play important roles in biogeochemical cycling and can act as plant growth-promoting bacteria by enhancing nutrient uptake [112,113]. As oligotrophic bacteria, their abundance tends to correlate negatively with soil nutrient enrichment [114]. Proteobacteria were most abundant in granite soils (24.42%) and least abundant in quartz schist soils (19.41%), which may reflect the potential association of soil geochemistry and other environmental factors with community structure [115]. Chloroflexi exhibited the highest abundance in quartz schist soils (13.18%) and the lowest in granite soils (9.17%). Members of this phylum are known to contribute to the natural degradation of organic pollutants via dehalogenation, participating in organic matter decomposition and nutrient cycling. Within this study, Chloroflexi abundance exhibited potential negative correlations with soil pH and a positive association with soil organic matter (SOM) content [116]. The relatively low abundance of Chloroflexi in granite soils may be linked to the higher feldspar content, which potentially influences their growth [117].

Other notable phyla include Planctomycetes, enriched in granite soils (5.89%) and positively correlated with soil Ca^{2+} content [118]; Gemmatimonadetes, most abundant in quartz schist soils (3.77%); and Actinobacteria, enriched in sericite schist soils (3.01%), likely linked to elevated soil As content. Actinobacteria can produce secondary metabolites such as siderophores, exhibiting strong As-binding capacity [119]. Nitrospirae was least abundant in sericite schist soils (0.03%), a trend potentially attributable to lower SOM content, which is often associated with Nitrospirae abundance [120]. Armatimonadetes were more abundant in sericite schist soils (1.28%) than quartz schist soils (0.57%), reflecting their aerobic chemoheterotrophic bacterial lifestyle and negative association with SOM [121].

Bacteroidetes and Verrucomicrobia displayed relatively low abundance across all soils, possibly due to their preference for alkaline soils and sampling depth effects [122,123].

Functional classification of bacterial communities revealed five major functional groups (Figure 2d): Gram-negative bacteria, biofilm-forming bacteria, potential pathogens, aerobic bacteria, and stress-tolerant bacteria, collectively representing over 90% of the total community. Gram-negative bacteria are broadly distributed and are recognized to participate in organic matter degradation, biological nitrogen fixation, and trace element transformation, playing essential roles in soil N cycling and plant-microbe interactions [124]. Biofilm-forming bacteria can influence soil aggregate structure and trace element degradation by enhancing microbial stress resistance. Their secretion of extracellular polymeric substances (EPS) often confers distinct ecological advantages, facilitating microbial growth, mineral aggregation and weathering, as well as ion exchange, complexation, and chelation processes. Potential pathogens may pose threats to crop health [125]. Aerobic bacteria rely on oxygen and perform key ecological functions in toxic environments. Stress-tolerant bacteria may contribute to plant growth regulation and resistance to environmental stress, often carrying antibiotic resistance genes (ARGs) and metal resistance genes (MRGs), highlighting the potential associations between trace elements and microbial communities [126,127].

3.3.2. Exploratory Analysis of Soil Geochemistry on Bacterial Community Distribution

This study suggested that soils derived from all three lithologies in the tea plantations exhibited trace element enrichment. Trace elements may exert dual effects on plant and microbial systems: at low concentrations, metals such as Zn, Cu, Fe, Mn, and Ni can act as essential micronutrients in metabolic processes, whereas elevated concentrations beyond biological tolerance thresholds might impose stress on plants and microbes [128]. Specifically, these trace elements appeared associated with potential effects on biological systems, primarily characterized by: potentially interfering with the uptake and translocation of essential macronutrients in tea plants, potentially leading to nutrient deficiency and imbalance [129]; potentially affecting cellular structures—including membranes and organelles—which might influence enzymatic activities, and destabilizing nucleic acid integrity, thereby possibly limiting cellular viability and hindering plant growth and development [130–132]; and associating with a shift in the diversity of soil microbial communities [133]. Exploratory analysis (Figure 3) highlighted several statistically significant associations between trace elements and major elements among soils derived from different lithologies. Importantly, as these patterns emerge from a small dataset, these associations are not definitive and may be sensitive to site-specific effects. In granite soils, Hg was significantly negatively correlated with Ca and Mg. It has been suggested that both Ca and Mg can accumulate on bacterial sheaths, potentially inhibiting plant uptake of Hg. In acidic soils, microbial activity and rhizosphere exudates might reduce Hg into bioavailable Hg^{2+}, which may compete with Ca^{2+} and Mg^{2+} for adsorption sites and transport proteins, thereby potentially influencing their bioavailability in the plant rhizosphere [40,134,135]. Gram-negative bacteria, which often exhibit high tolerance to Hg, showed the greatest relative abundance across all samples [13,136,137]. In quartz schist soils, Cr showed a strong negative correlation with Al, and potential synergistic effects of Pb and Cr were associated with suppressed SOM degradation, which appeared linked to reduced net microbial biomass accumulation [138]. Sericite schist soils exhibited more complex potential stress relationships, where Zn and As were negatively correlated with Ca, and Mn was negatively correlated with Al. Under acidic conditions ($pH < 5.5$), limited availability of K, Ca, and Mg may exacerbate nutrient deficiency [139].

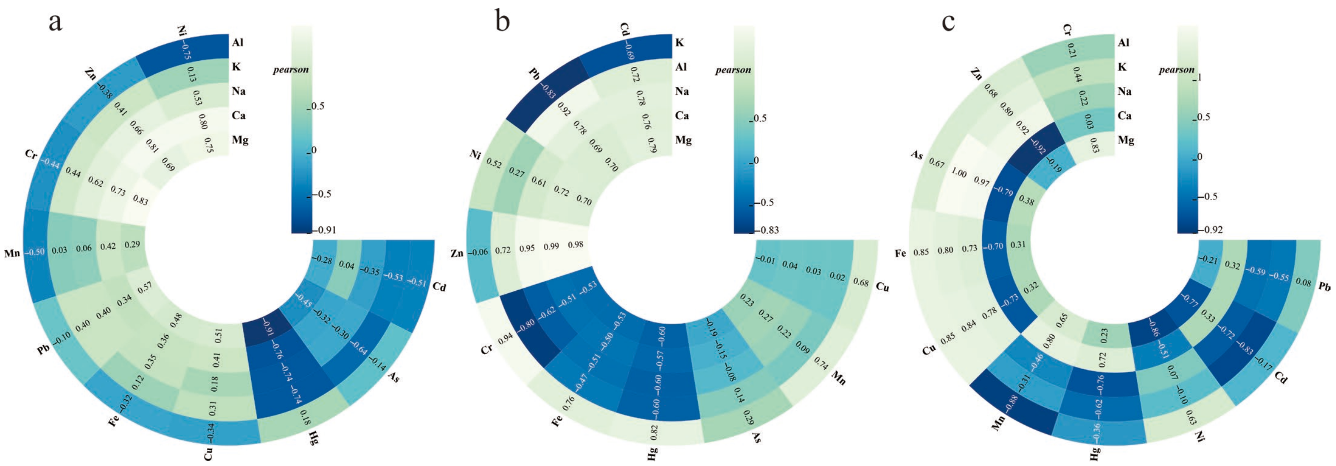

Figure 3. Exploratory correlation heatmap and hierarchical clustering of major and trace elements in soils across different lithologies. (**a**) GT, (**b**) QS, (**c**) SS. Colors represent the magnitude and direction of Pearson correlation coefficients.

Potential competitive substitution between nutrient ions and trace elements [140] may further influence the bioavailability of Zn and As. Tea plants, as an Al-tolerant crop, may resist Al toxicity through plant-microbe synergistic mechanisms in acidic soils enriched with Al-tolerant microbes [141,142]. Moreover, a potential antagonism between Mn and Al appeared evident: Mn potentially influences Al uptake and utilization, while associating with changes in root architecture and nutrient acquisition efficiency [143,144]. Soil microbes likely not only endure trace element stress but may also contribute to mitigating its toxicity, thereby potentially supporting ecosystem stability. Plant growth-promoting bacteria (PGPB) in soils and rhizospheres were associated with enhanced tea plant tolerance [145–147]. While Zn, Ni, and Cu may suppress microbial respiration—with potential additive or synergistic toxic effects—PGPB potentially counteract toxicity through mechanisms including metal chelation, biosorption, and secretion of extracellular polymeric substances (EPS) [148,149]. For instance, under acidic conditions with elevated H^+ concentrations, exchangeable sites on soil particles can be competitively occupied by H^+, thereby potentially limiting the availability of exchangeable K^+. Potassium-solubilizing bacteria (KSB) appeared capable of releasing soluble K from insoluble K-bearing minerals (e.g., feldspars), even under Fe stress, potentially maintaining K supply for plant uptake [150].

To further investigate the potential interactions between geochemical elements and microbial communities, exploratory Redundancy Analysis (RDA) was performed following a detrended correspondence analysis (DCA). Since the first axis lengths were <3, RDA was employed (Figure 4) as an exploratory visualization tool to illustrate potential relationships between bacterial communities and soil geochemical properties across different lithological regions. The text should make it clear that these ordinations serve to organize patterns within the dataset, and individual relationships should not be treated as independently confirmed. The two axes explained 95.47%, 95.35%, and 94.98% of the variance in bacterial community composition for the granite (Figure 4a), quartz schist (Figure 4b), and sericite schist (Figure 4c) soils, respectively. In the granite soils, Acidobacteria and Chloroflexi appeared to track positively with the chemical index of weathering (CIW), Hg, and Al, while showing potential negative associations with Na, Zn, Mn, Mg, pH, Ca, Cd, Cu, Cr, and Ni. Conversely, Nitrospirae, Gemmatimonadetes, Proteobacteria, Bacteroidetes and Verrucomicrobia generally exhibited contrasting trends, showing associations opposite to those of Acidobacteria and Chloroflexi. In the quartz schist soils, Acidobacteria showed positive associations with CIA and CIW, but appeared to correlate negatively with Ni, Zn, Ca, Mg, Na, Al, and pH. In contrast, Actinobacteria, Bacteroidetes, Verrucomicrobia, candidate division WPS-1, Planctomycetes, and Armatimonadetes exhibited opposite patterns and showed potential negative associations with Acidobacteria. Additionally, Chloroflexi were associated with CIA, Cd, and Pb, but showed inverse trends with WIP, Mn, Cu, K, As, Cr, Fe, Hg, and SOM. Proteobacteria, Gemmatimonadetes, and Nitrospirae exhibited potential inverse correlations and showed negative associations with Chloroflexi. In the sericite schist soils, Acidobacteria showed positive associations with Mg, Mn, and SOM, but appeared to correlate negatively with Cr, Ni, pH, CIW, Fe, Al, and Cu. By contrast, Nitrospirae, Gemmatimonadetes, Armatimonadetes, Bacteroidetes, and Verrucomicrobia displayed opposite associations and showed potential negative associations with Acidobacteria. Furthermore, Proteobacteria and Planctomycetes exhibited potential positive associations with Hg, Cd, Pb, and CIA, but showed inverse trends with WIP, K, As, Zn, and Na, while Chloroflexi and Actinobacteria exhibited the reverse trends and showed negative associations with Proteobacteria and Planctomycetes.

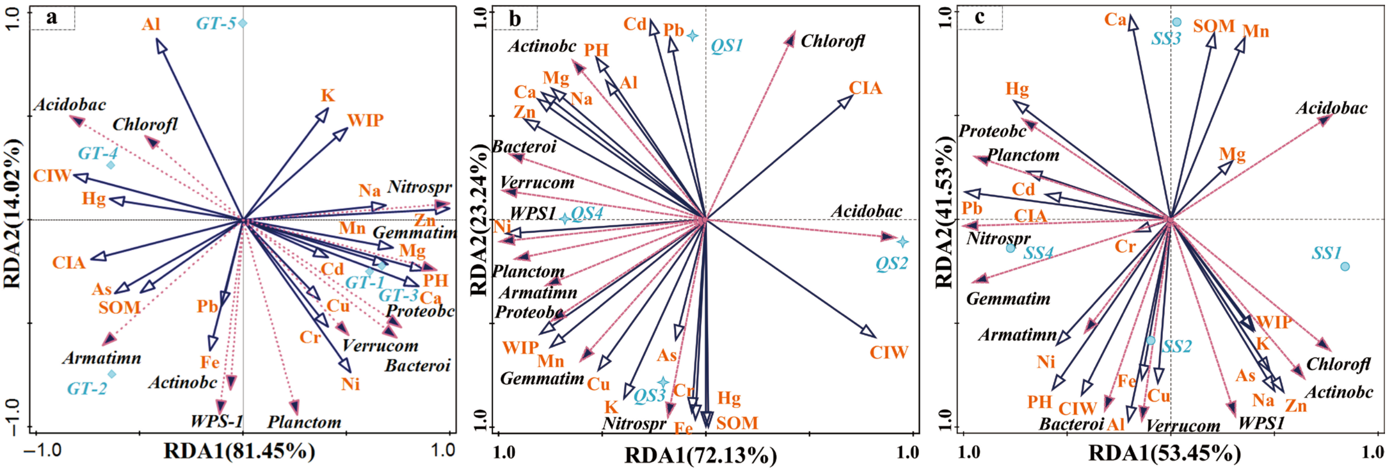

Figure 4. Exploratory two-dimensional Redundancy Analysis (RDA) ordination plot of soil properties and bacterial communities. The length of a soil property ray indicates its relative magnitude of association with the bacterial community. Correlations are represented by the angle between vectors: an acute angle indicates a positive correlation, while an obtuse angle indicates a negative correlation. (**a**) GT, (**b**) QS, (**c**) SS.

Exploratory Pearson correlation analysis between soil geochemistry and bacterial phyla with relative abundances >0.5% was further conducted, with results visualized as a correlation heatmap (Figure 5). Similarly to the ordinations, these visualizations highlight candidate relationships rather than definitive mechanisms. In granite soils, Verrucomicrobia correlated positively with Ni, Cr, and Cu but negatively with Hg; Bacteroidetes and Proteobacteria correlated positively with pH and Ca but negatively with CIW; Actinobacteria correlated negatively with K; Gemmatimonadetes correlated positively with Mn and Zn; Nitrospirae correlated positively with pH, Ca, and Zn; Chloroflexi appeared strongly negatively associated with Cu and negatively correlated with Cr; while Acidobacteria correlated positively with CIW but negatively with pH and Ca. Overall, pH, Ca, and CIW appeared to exhibit the strongest potential associations with bacterial communities in GT soils. In quartz schist soils, Proteobacteria correlated positively with WIP but negatively with CIA; Planctomycetes correlated positively with Ni and WIP; Nitrospirae correlated positively with K and Cr; Gemmatimonadetes correlated positively with Cu and Mn. Notably, Actinobacteria exhibited significant positive correlations with pH, Ca, Na, and Mg, potentially reflecting an adaptation to specific geochemical niches [151]. Bacteroidetes correlated positively with Zn; Armatimonadetes correlated negatively with CIA; and Verrucomicrobia correlated positively with Zn. SOM, Ni, and Hg showed the most noticeable potential associations with microbial composition in quartz schist soils. In sericite schist soils, Proteobacteria correlated positively with Cd and CIA; Chloroflexi correlated negatively with Pb; Planctomycetes correlated positively with Pb; Actinobacteria correlated positively with Zn but negatively with Hg; Bacteroidetes correlated positively with pH and CIW but negatively with Mn; candidate division WPS-1 correlated positively with Zn and Na but negatively with Ca; and Verrucomicrobia correlated positively with Al, Fe, and Cu but strongly negatively with SOM. Al, Ca, Zn, and Na were the primary factors associated with microbial assemblages in sericite schist soils.

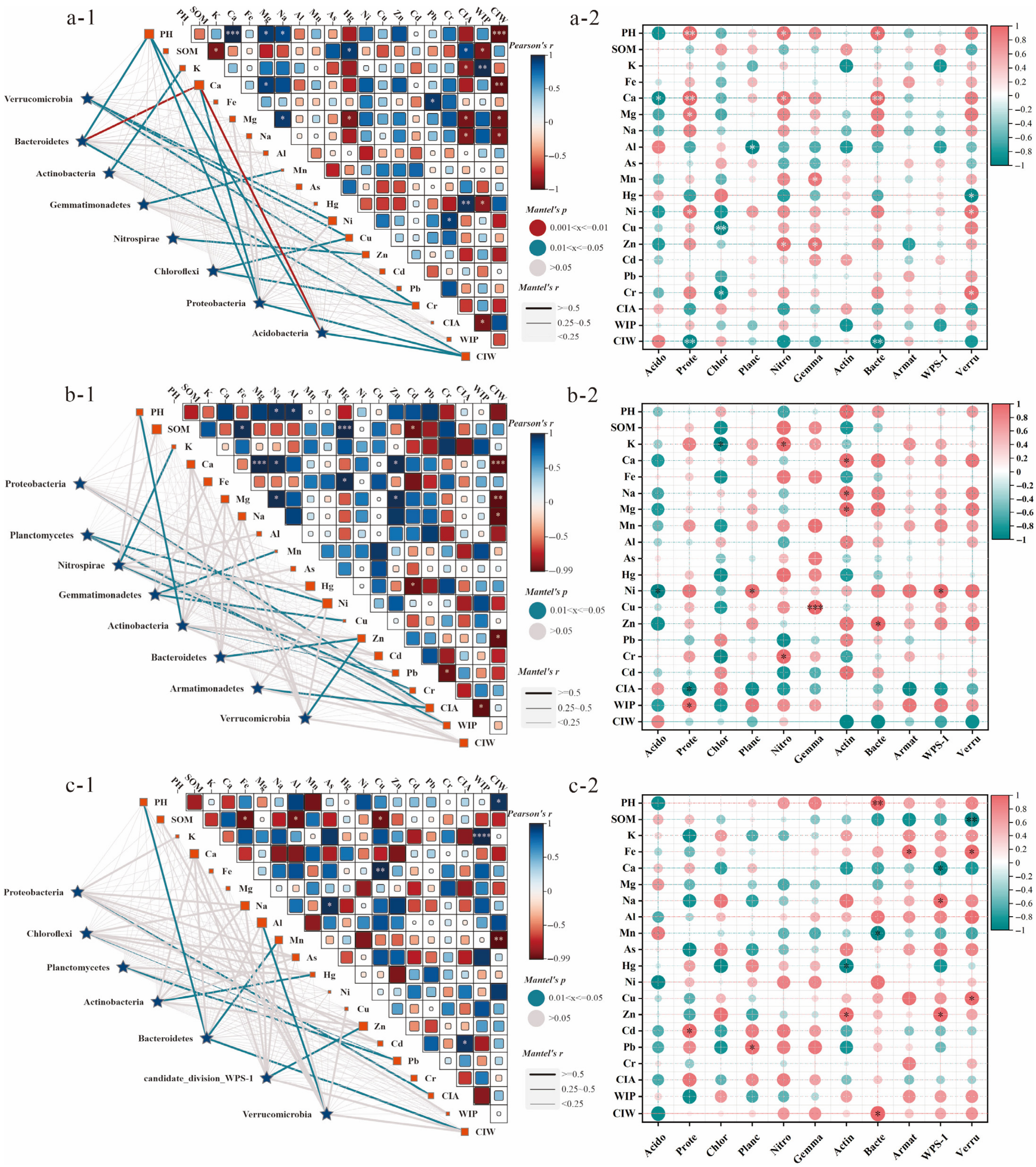

Figure 5. Exploratory analysis of potential relationships between soil geochemical properties and bacterial communities in (**a**) GT, (**b**) QS, and (**c**) SS. Left panels (**a-1**,**b-1**,**c-1**): Correlation network

correlation coefficients (r) between environmental factors. The width and color of the connecting lines represent Mantel's statistic (r) and significance (p) values, respectively. Right panels (**a-2**,**b-2**,**c-2**): Correlation heatmap between environmental factors and dominant bacterial phyla. Red and blue/teal represent positive and negative correlations, respectively. The size of the squares is proportional to the absolute value of the correlation coefficient. * $p < 0.05$, ** $p < 0.01$, ***$p < 0.001$, **** $p < 0.0001$. Abbreviations: Acido, Acidobacteria; Prote, Proteobacteria; Chlor, Chloroflexi; Nitro, Nitrospirae; Gemma, Gemmatimonadetes; Actin, Actinobacteria; Bacte, Bacteroidetes; Armat, Armatimonadetes; WPS-1, candidate_division_WPS-1; Verru, Verrucomicrobia.

Under trace element stress, the geochemical characteristics of soils developed from different rock types and the responses of soil microbial communities exhibit marked lithological differences. Certain soil bacterial communities appear potentially influenced by abiotic drivers, such as weathering, with microorganisms mediating mineral weathering processes and influencing ion cycling as well as plant nutrient availability [152,153]. In acidic environments, competitive adsorption occurs between trace elements and major elements. Rhizosphere bacteria of tea plants may absorb and immobilize trace elements, thereby potentially reducing their translocation to aboveground plant tissues, while simultaneously secreting chelating agents (such as organic acids and amino acids), which may enhance the solubility and bioavailability of major elements in the soil. Under trace element stress, soil bacterial communities appear to play multiple critical roles, both responding to elemental toxicity and potentially mitigating its detrimental effects through diverse physiological mechanisms.

3.4. Migration and Enrichment Characteristics of Elements in the Rock–Soil–Tea Ecosystem

Significant differences were observed in the concentrations of Fe, Mn, and Cu in tea leaves across the three lithological regions (Table 5). Fe concentrations were highest in tea leaves developed on quartz schist and lowest in those on granite, whereas Mn and Cu were most enriched in tea leaves from sericite schist plantations. The migration of elements from parent rock to tea leaves involves three primary stages: rock weathering, soil retention, and plant uptake. During weathering, readily soluble elements are preferentially released and consumed, while less soluble elements become sequestered in the surface soil [154], often forming stable phases through association with secondary iron oxides [102]. Nutrient uptake by tea roots is further influenced by selective absorption mechanisms that modulate the entry of elements into the leaves.

Table 5. Elemental content in tea from different lithological areas.

Tea	GT	QZ	SS	F	p
K	4.137 ± 0.071^{a}	4.063 ± 0.384^{a}	4.606 ± 0.156^{a}	1.645	0.133
Ca	0.94 ± 0.072^{a}	0.814 ± 0.098^{a}	0.924 ± 0.152^{a}	0.402	0.446
Fe	0.008 ± 0^{a}	0.055 ± 0.028^{a}	0.01 ± 0.001^{a}	3.019	0.061
Mg	0.459 ± 0.034^{a}	0.404 ± 0.015^{a}	0.434 ± 0.005^{a}	1.303	0.161
Na	0.004 ± 0.0004^{a}	0.004 ± 0.0001^{a}	0.009 ± 0.005^{a}	1.529	0.164
Al	0.097 ± 0.026^{a}	0.107 ± 0.029^{a}	0.131 ± 0.019^{a}	0.474	0.389
Mn	0.049 ± 0.007^{b}	0.061 ± 0.008^{b}	0.102 ± 0.013^{a}	8.532	0.007
As	0.067 ± 0.011^{a}	0.091 ± 0.02^{a}	0.084 ± 0.02^{a}	0.564	0.362
Hg	0.003 ± 0.0004^{a}	0.004 ± 0.0004^{a}	0.003 ± 0.001^{a}	1.456	0.127
Ni	4.402 ± 0.646^{a}	4.752 ± 0.525^{a}	4.49 ± 0.424^{a}	0.103	0.686
Cu	13.444 ± 1.122^{b}	16.629 ± 0.845^{a}	16.7 ± 0.776^{a}	3.898	0.056
Zn	21.1 ± 1.009^{a}	23.245 ± 1.789^{a}	24.175 ± 1.14^{a}	1.525	0.146
Cd	0.034 ± 0.017^{a}	0.01 ± 0.004^{a}	0.036 ± 0.011^{a}	1.148	0.216
Pb	0.102 ± 0.011^{a}	0.221 ± 0.075^{a}	0.238 ± 0.063^{a}	2.124	0.112
Cr	0.518 ± 0.096^{a}	1.353 ± 0.731^{a}	1.21 ± 0.26^{a}	1.238	0.205

Values are expressed as mean ± SD. Significant differences ($p < 0.05$) determined by one-way ANOVA followed by an LSD test are indicated by different lowercase letters within the same row. Units: %, for K, Ca, Mg, Fe, Al, Na, and Mn; $mg \cdot kg^{-1}$, for Cu, Zn, Cr, Pb, Cd, Hg, Ni, and As.

The relationship between the Enrichment Factor (EF) and the bioconcentration factor (BCF) provides preliminary insight into the migration behavior of both major and trace elements within the rock–soil–tea ecosystem. As shown in Table 6, elements such as Hg, Pb, Al, Ca, Mn, Zn, and Cr tend to be relatively enriched during the transition from parent rock to soil. K, Ca, Mg, and Mn exhibit stronger enrichment advantages during the soil-to-tea transfer. Hg and Pb form complexes with soil Fe-Mn oxides and soil organic matter (SOM) [155], while Al stabilizes within aluminosilicate and aluminate minerals [156], potentially leading to their sequestration in surface soils with minimal leaching and negligible accumulation in tea leaves. In comparison, K, Ca, and Mn display strong enrichment in tea leaves, with a consistent sequence of Ca > K > Mn > Mg across all lithologies. Ca is mainly localized within plant cells in relatively high concentrations, whereas Mg primarily occurs as a structural component of chlorophyll in tea plants [157]. By contrast, major elements such as Na and Al, as well as trace elements including Cu, Zn, Pb, Cr, Cd, Hg, Ni, and As, exhibit negligible enrichment in tea leaves. Lithology strongly influences the primary chemical composition of soils, whereas elemental enrichment in tea leaves is predominantly associated with the metabolic demands of tea plants and the interplay of antagonistic and synergistic interactions among elements. For instance, in the sericite schist region (Figure 3c), Ni and Mg exhibit a significant negative correlation, potentially reflecting competitive inhibition between the two elements [158]. Under the selective uptake mechanisms of tea roots, the BCF of Mg is substantially greater than that of Ni. Antagonistic interactions are also evident in the potential interference of Mg with the translocation and accumulation of Cd [159,160]. By contrast, potential synergistic effects are observed in the granite region (Figure 4a), where Zn shows significant positive correlations with essential elements for tea growth, including K, Ca, Na, and Mg [161].

Table 6. Mean values of the enrichment factor (EF) and bioconcentration factor (BCF) across different lithological groups.

Group	GT		QZ		SS	
	EF	BCF	EF	BCF	EF	BCF
K	0.9028	2.3525	0.4568	2.7830	0.6043	3.1996
Ca	1.7332	15.2367	1.0159	14.0078	0.5827	13.1813
Fe	1.2396	0.0020	0.8938	0.0105	0.7644	0.0025
Mg	0.9459	0.6774	0.7013	0.7727	0.3427	1.1517
Na	0.4640	0.0479	0.9168	0.0920	0.1997	0.5058
Al	1.0000	0.0106	1.0000	0.0116	1.0000	0.0158
Mn	2.1009	1.1471	1.4211	0.9391	0.5040	3.6064
As	0.6108	0.0089	0.9434	0.0072	2.3247	0.0062
Hg	8.9955	0.0620	6.8973	0.0388	3.4704	0.0775
Ni	1.8024	0.1346	0.8229	0.1148	0.6868	0.1675
Cu	0.1717	0.5761	0.3164	0.4652	0.2659	0.7944
Zn	1.9498	0.2840	1.1036	0.2872	0.7685	0.4448
Cd	0.6822	0.5265	0.3137	0.2523	0.3732	0.8295
Pb	3.5252	0.0036	2.9276	0.0061	4.6239	0.0097
Cr	1.5753	0.0065	0.8801	0.0107	1.0533	0.0146

An EF value > 1 indicates relative enrichment of the element in the soil compared to the parent material, while a value < 1 signifies leaching or depletion. A higher BCF value denotes a stronger accumulation capacity of the tea plant for the respective element.

Further exploratory correlation heatmap analysis (Figure 6) provided insights into the potential dynamics underlying EF, BCF and mineral associations within the rock–soil–tea ecosystem. SOM showed a significant positive correlation with the EF of Hg but a negative correlation with its BCF. SOM forms stable organo-Hg complexes with Hg^{2+} in the soil, thereby potentially suppressing its mobility and bioavailability [162].

Montmorillonite was significantly positively correlated with the BCF of Pb and Mn, while kaolinite showed significant positive associations with the BCF of Mg and Cu. This likely reflects their differential capacities to accumulate specific elements, while acidic conditions may disrupt surface complexes between clay minerals and trace elements and enhance Mn bioavailability [163,164]. Soil pH exhibited a significant positive correlation with the EF of Ca but a negative correlation with its BCF, as lower pH increases Ca^{2+} solubility and bioavailability while reducing its retention in soils [165]. Additionally, K-feldspar and plagioclase were significantly positively correlated with the EF of Zn and Cr, whereas biotite correlated significantly primarily with the EF of Zn. These associations are potentially attributable to the weathering of these minerals into clay minerals (such as montmorillonite and kaolinite) that effectively adsorb Zn^{2+} and Cr^{3+} [166,167]. Finally, the chemical index of alteration showed significant positive correlations with the BCF of K and Mg, suggesting that progressive rock weathering enhances the release of K^+ and Mg^{2+}, thereby facilitating their uptake by tea plants [168].

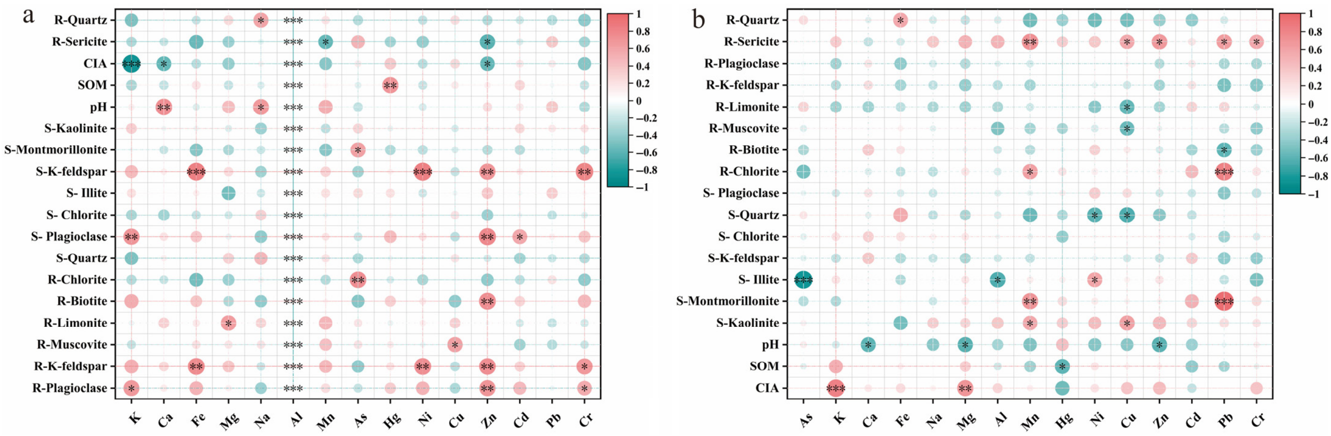

Figure 6. Exploratory correlation heatmaps of environmental factors with (**a**) enrichment factor (EF) and (**b**) bioconcentration factor (BCF). Red and blue/teal indicate positive and negative correlations, respectively. Circle size corresponds to the absolute correlation coefficient (r). Asterisks indicate significance: * $p < 0.05$, ** $p < 0.01$, *** $p < 0.001$.

4. Discussion

4.1. Potential Interactive Mechanisms Between Soil Bacterial Communities and Elemental Migration in the Rock–Soil–Tea Ecosystem

4.1.1. Rock-to-Soil Elemental Migration and Bacterial Communities Interaction Mechanisms

The migration and enrichment of elements from bedrock to soil provide essential habitat conditions that sustain soil microbial communities [169]. During weathering, the dissolution and transformation of primary minerals release nutritive elements that fuel bacterial growth, reproduction and metabolism, while bacterial metabolic products in turn enhance rock decomposition and element mobilization, forming what may be a positive feedback loop between mineral weathering and microbial activity [170]. To explore the potential mineral–element–microbe interaction mechanisms, an exploratory correlation analysis of soil minerals, rock minerals, and the enrichment factor was performed, with significant correlations ($p < 0.05$) visualized using chord diagrams (Figure 7a–c). To further dissect the complex relationships among microbial diversity, rock/soil/tea elemental contents and bacterial abundances, network diagrams (Figure 7d–f) were constructed. Bacterial community α-diversity was quantified using the Shannon index.

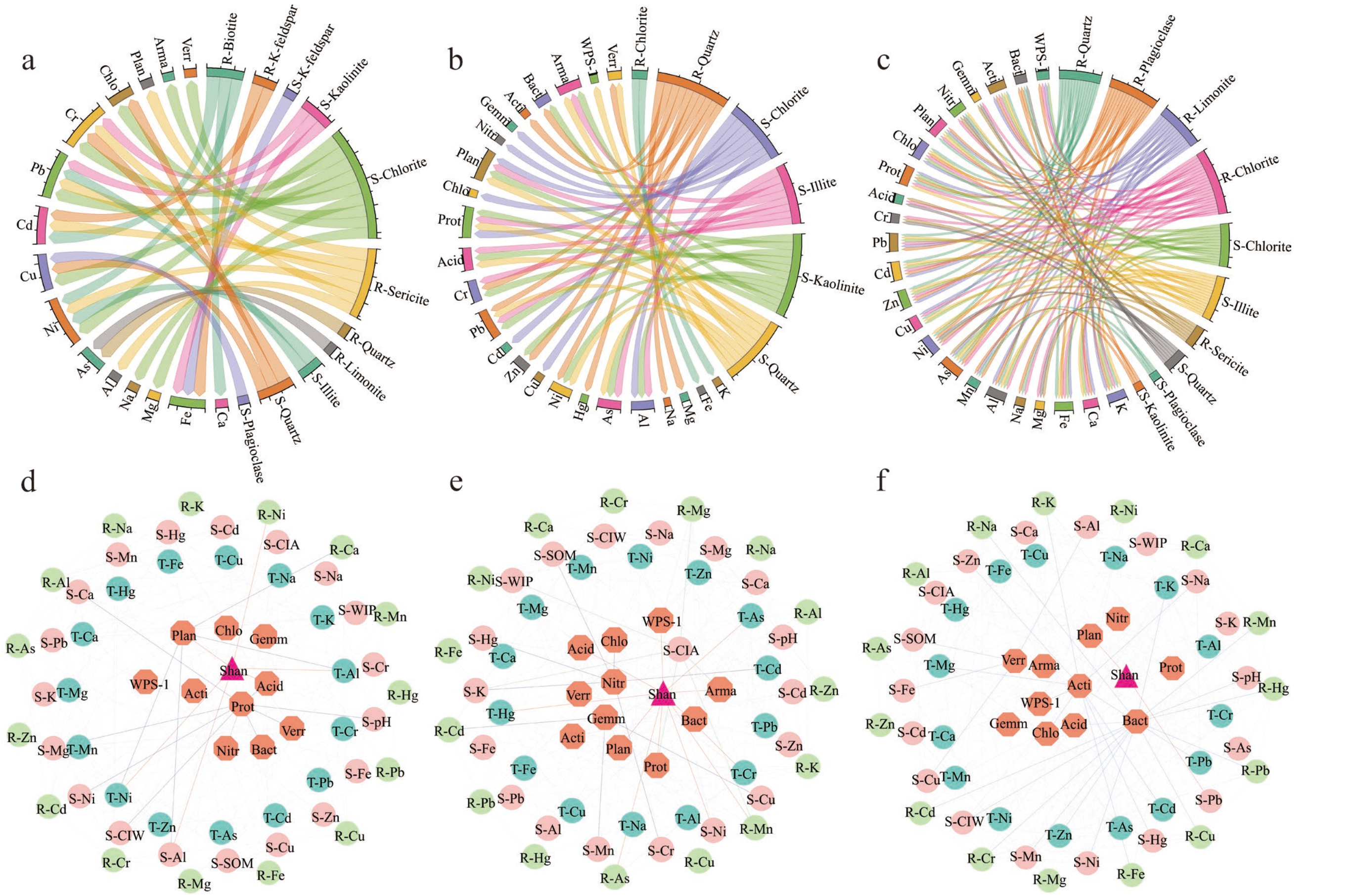

Figure 7. Exploratory chord diagrams (**a**–**c**) and network analysis diagrams (**d**–**f**) illustrating potential associations among soil minerals, elements, and the top 11 most abundant bacterial phyla across different lithologies: (**a**,**d**) Granite (GT), (**b**,**e**) Quartz schist (QS), and (**c**,**f**) Sericite schist (SS). Only statistically significant correlations ($p < 0.05$) are displayed. Abbreviations: R, rock elements; S, soil elements; T, tea elements. Bacterial phyla abbreviations: Acid, Acidobacteria; Prot, Proteobacteria; Chlo, Chloroflexi; Nitr, Nitrospirae; Gemm, Gemmatimonadetes; Acti, Actinobacteria; Bact, Bacteroidetes; Arma, Armatimonadetes; WPS-1, candidate_division_WPS-1; Verr, Verrucomicrobia; Late, Latescibacteria.

In granite soils (Figure 7a,d), chlorite exhibited the most prominent potential association with both element migration and bacterial abundance. By potentially modulating the migration and enrichment behavior of Cr, Pb, Cu, Ni, Mg and Na, chlorite was associated with shifts in the relative abundances of phyla such as Verrucomicrobia, Armatimonadetes and Chloroflexi. Al and Ni, through their respective associations with Acidobacteria and Planctomycetes, were also associated with variations in bacterial α-diversity. Soils developed on granite contained higher concentrations of Mg and Na than the other lithologies (Table 2), and exhibited greater enrichments of Cr, Pb, and Ni (Table 6). Such elemental patterns appear to selectively influence the relative abundance of specific bacterial taxa. Chloritization and associated alteration processes can alter the mobility of trace elements (e.g., Cr, Pb, Cu, Ni), thereby potentially influencing soil bacterial community structures, including Verrucomicrobia and Chloroflexi [171–173]. Meanwhile, extracellular polymeric substances (EPS) secreted by soil bacteria regulate microbial attachment to solid surfaces (e.g., clay minerals), which in turn may modulate mineral aggregation and weathering processes [174]. The correlation heatmap (Figure 5a) indicated positive associations of Al with Acidobacteria and of Ni with Planctomycetes. Acidobacteria appear advantaged in low-pH, Al-enriched conditions. Planctomycetes possess a complex intracellular membrane system, whose compartmentalized architecture provides a potential mechanism for trace element sequestration. This unique structural adaptation may enable them to tolerate Ni stress in ways that distinguish them from other bacterial taxa [175], likely explaining their sustained abundance in Ni-rich granite soils. Together, Acidobacteria and Planctomycetes may act as candidate keystone taxa potentially contributing to the maintenance of high bacterial diversity in the granite soil (Table 4).

In quartz schist soils (Figure 7b,e), kaolinite showed notable candidate associations with the mobility of Pb, Cr, Ni, Zn and As and thus correlated with the relative abundances of Planctomycetes, Proteobacteria and Acidobacteria. In addition to Cr and Ni, Mn and Hg also correlated with the α-diversity of soil bacterial communities. The potential mineral–element–microbe interaction is hypothesized as follows: kaolinite adsorbs Pb, Cr, Ni and Zn through ion exchange and surface complexation [176], reducing their mobility and bioavailability in soils [177]. Microbial processes such as biomineralization can in turn affect mineral dissolution and precipitation, thereby altering the migration and enrichment of trace elements such as Pb, Ni and As [178,179]. Quartz schist soils displayed the highest concentrations of Cr, Ni, Mn and Hg (Table 2). The correlation heatmap (Figure 5b) shows that Mn, Ni and Cr correlate negatively with Acidobacteria but positively with Proteobacteria, suggesting that high Mn, Ni and Cr levels potentially suppress sensitive taxa (e.g., Acidobacteria) while favoring tolerant groups (e.g., Proteobacteria). Hg correlated positively with both Acidobacteria and Proteobacteria, indicating taxon-specific tolerances and adaptive responses to different trace elements [180]. Planctomycetes displayed correlation patterns with Ni similar to those observed in the granite soils. Nitrospirae and Gemmatimonadetes reached their highest abundances in quartz schist soils; these taxa participate in complex nutrient cycling and organic matter degradation, thereby contributing to α-diversity. Nitrospirae showed positive associations with K, Cr and Hg, and K potentially promoted bacterial growth through ion exchange. As metal-resistant microorganisms (MRMs), Nitrospirae can activate metal resistance genes (MRGs) under Cr and Hg stress, enabling survival in contaminated soils [181]. Gemmatimonadetes correlated positively with Mn and Cu, potentially reflecting links between their metabolism and Mn oxidation [182,183]. Given that weathering intensity is greatest in the quartz schist region, we examined relationships between weathering indices and bacterial community composition. The chemical index of alteration correlated notably with K, Mg, Armatimonadetes and Proteobacteria. Both K and Mg are progressively leached during weathering (Table 6), and the negative relationship between K/Mg and CIA observed in the RDA (Figure 4b) is consistent with the observation that the contents of K and Mg decreased as the degree of weathering increased 120 [184]. Correspondingly, the relative abundances of Armatimonadetes and Proteobacteria were negatively correlated with CIA, potentially explaining their lower abundances in highly weathered quartz schist soils [185].

The sericite schist region exhibited complex potential mineral-microbe associations (Figure 7c,f). Clay minerals (chlorite, plagioclase, goethite and illite) showed strong correlations with the migration and enrichment of Pb, K, Ca, Cd, As, Al, Fe and Zn, thereby associating with the abundances of Actinobacteria, Planctomycetes, Chloroflexi and Proteobacteria. In particular, Pb exhibited a major association with Planctomycetes and hence with bacterial α-diversity. Feldspars are the primary source of soil K, and Actinobacteria—known to promote tea plant growth and enhance their resistance to pathogens and environmental stress—can solubilize mineral-bound K, potentially explaining the relatively high Actinobacteria abundance observed in sericite schist soils [186]. The hypothesized mineral–element–microbe interaction is as follows: plagioclase surfaces adsorb trace element ions (e.g., Pb^{2+}, Cd^{2+}, Zn^{2+}), while exchangeable cations on these surfaces (mainly Ca^{2+}, Na^{+}) undergo ion-exchange reactions with trace elements in solution, thereby potentially influencing metal migration and enrichment [187,188]. Illite can lower the bioavailability of Pb, Cd, Zn and Ni via ion adsorption and fixation, and its cation exchange capacity regulates Ca and K mobility, with potential downstream effects on bacterial abundance and diversity [174]. Concurrently, bacterial attachment and metabolic activities alter mineral dissolution behavior [189,190]. Actinobacteria and Proteobacteria secrete soluble organic acids that complex Al and Fe, thereby promoting the weathering of feldspars and related minerals [117]. Actinobacteria additionally reduce Fe^{3+} to Fe^{2+}, facilitating the dissolution of Fe-oxides such as limonite [191,192]; their Fe-reduction process is also implicated in the formation and transformation of illite [193]. Siderophores secreted by Actinobacteria chelate Fe^{3+} to form highly stable complexes, substantially enhancing the Fe bioavailability to tea plants [194]; Fe-induced respiratory activity further strengthens Actinobacteria's antibiotic resistance, while elevated Fe concentrations stimulate their metabolic activity and sustain energy supply under anoxic conditions [195]. Actinobacteria mobilize Zn through siderophores and other metabolites, enabling them to dominate Zn-enriched tea rhizosphere soils and promoting Zn uptake by tea plants [196,197]. Proteobacteria correlated positively with Cd (Figure 5c) and can mitigate Cd stress by activating antioxidant enzyme systems and by secreting extracellular polymeric substances (EPS) that immobilize Cd as insoluble complexes, thereby reducing its bioavailability and toxicity [198,199]. Pb was enriched in sericite schist soils and exhibited a significant positive correlation with Planctomycetes (Figure 5c). Pb was associated with bacterial functional diversity more strongly than species diversity, suggesting that its ecological impact may be mediated primarily through shifts in bacterial functional traits, with potential consequences for ecosystem stability [200].

Collectively, distinct geological settings exhibit divergent geochemical cycling patterns and microbial community responses. Clay minerals can regulate the distribution and mobility of major elements and trace elements through ion adsorption and cation exchange while simultaneously providing energy sources and microhabitats for microbial metabolism. The hypothesized response mechanisms of soil microbial communities can be summarized as follows: secretion of organic acids to promote mineral weathering and element release; production of EPS to mitigate trace element toxicity under stress; and synthesis of siderophores to enhance competitiveness under Fe limitation and to chelate other metals. Bacteria possess a strong protein-degrading capacity, enabling them to participate critically in organic matter decomposition and elemental cycling. Among them, Verrucomicrobia not only exhibit notable trace-element tolerance [201] but also display a strong negative correlation with SOM (Figure 5). As key decomposers of derivative organic matter, Verrucomicrobia preferentially degrade xylan-type hemicellulose within SOM [202]. The synthesis of metalloproteins strongly influences the bacterial capacity for trace element adsorption, accumulation, and detoxification. For instance, bacteria can immobilize Cr^{3+}, Zn^{2+}, Cu^{2+}, and Cd^{2+} ions at the cell surface by producing metallothioneins or metal-binding peptides, thereby substantially reducing both the toxicity and mobility of trace elements [203–205]. Driven by specific key elements and microbial functions, mineral-element-microbe interactions in the study area tend to form integrated network structures. The presence of trace elements markedly alters microbial community composition, characterized by declines in sensitive taxa and the enrichment of tolerant taxa: sensitive groups suffer structural damage and reduced relative abundance, whereas metal-resistant taxa employ detoxification strategies, potentially becoming dominant and thereby contributing to observed shifts in community richness and evenness within this dataset.

4.1.2. Soil-to-Tea Leaves Elemental Migration and Bacterial Communities Interaction Mechanisms

Soil serves as a bridge for elemental translocation and enrichment, and these processes are associated with microbial community structure and distribution [206]. Conversely, shifts in microbial community composition potentially influence nutrient cycling, metal speciation, and rhizosphere interactions, ultimately affecting the uptake of both trace elements and major elements by tea plants. This bidirectional relationship between microbial communities and elemental migration constitutes a potential microbe-plant interaction network. To explore this relationship, exploratory redundancy analysis was performed on tea leaf elements and the bioconcentration factor (BCF) in relation to bacterial α-diversity (Figure 8). Consistent with the scale of this study, these analyses are intended to organize site-specific patterns rather than confirm definitive regulatory roles. The results revealed suggested that potential correlations between tea leaf elements, BCF, and bacterial community diversity varied across lithological settings. Elements such as K, Ca, Mn, and Mg were relatively enriched in tea leaves (Table 6), and thus their candidate interactions with bacterial α-diversity were further analyzed in detail. In granite and sericite schist tea plantations, K showed a consistent pattern: tea leaf K content correlated negatively with the bacterial α-diversity index, whereas its BCF correlated positively. By contrast, both relationships were negative in quartz schist tea plantations. Across all three lithologies, soil K showed leaching loss (Table 6), while tea leaf K was largely derived from soil. This suggests that in quartz schist regions, stronger K transfer to leaves potentially depletes soil K, thereby associating with reduced bacterial diversity [207,208]. Under conditions of a low soil bacterial Shannon index, a few highly efficient K-solubilizing taxa may become enriched, secreting organic acids to dissolve silicate minerals, thereby increasing soil K availability and promoting tea plant uptake. In granite and sericite schist soils, however, where K concentrations are inherently higher, sufficient K supply appears to support both tea growth and relatively high microbial diversity. Indeed, high-K rhizospheres have been linked to greater bacterial diversity [209], as the BCF of K increased, α-diversity was also maintained at a higher level.

For Ca and Mg, both granite and quartz schist soils showed similar patterns: the Shannon index was negatively correlated with tea leaf Ca and Mg concentrations as well as their BCF, suggesting that greater translocation of Ca and Mg from soil to leaves was accompanied by reduced α-diversity. Tea leaf Mn concentrations and their BCF were negatively correlated with the soil bacterial Shannon index across all three lithologies. Mn was enriched in both soil and tea leaves (Table 6), likely due to the ability of Mn-tolerant taxa to secrete enzymes such as multicopper oxidases and manganese reductases, which enhance Mn solubilization. These Mn-tolerant taxa may exhibit a survival advantage under Mn stress, potentially suppressing sensitive groups and thereby reducing overall bacterial community diversity [210].

In summary, geochemical variations across lithological tea plantations are associated with distinct candidate interaction patterns between elemental translocation and bacterial α-diversity within this dataset.

4.2. Factors Influencing Elemental Migration

The process of elemental translocation not only shapes soil microbial community structures but also potentially influences patterns of elemental accumulation in tea leaves. To explore the potential factors driving elemental migration within the rock–soil–tea ecosystem, an exploratory decision tree analysis was performed. In strict alignment with the localized, hypothesis-generating nature of this dataset, the detailed decision-tree (CART) results have been relocated to the Supplementary Material. Decision tree models have been widely applied in system modeling [211], with the Classification and Regression Tree (CART) approach being particularly notable. CART constructs a tree-like structure for data classification and heuristic exploration by recursively splitting attributes into binary categories based on class labels [212,213].

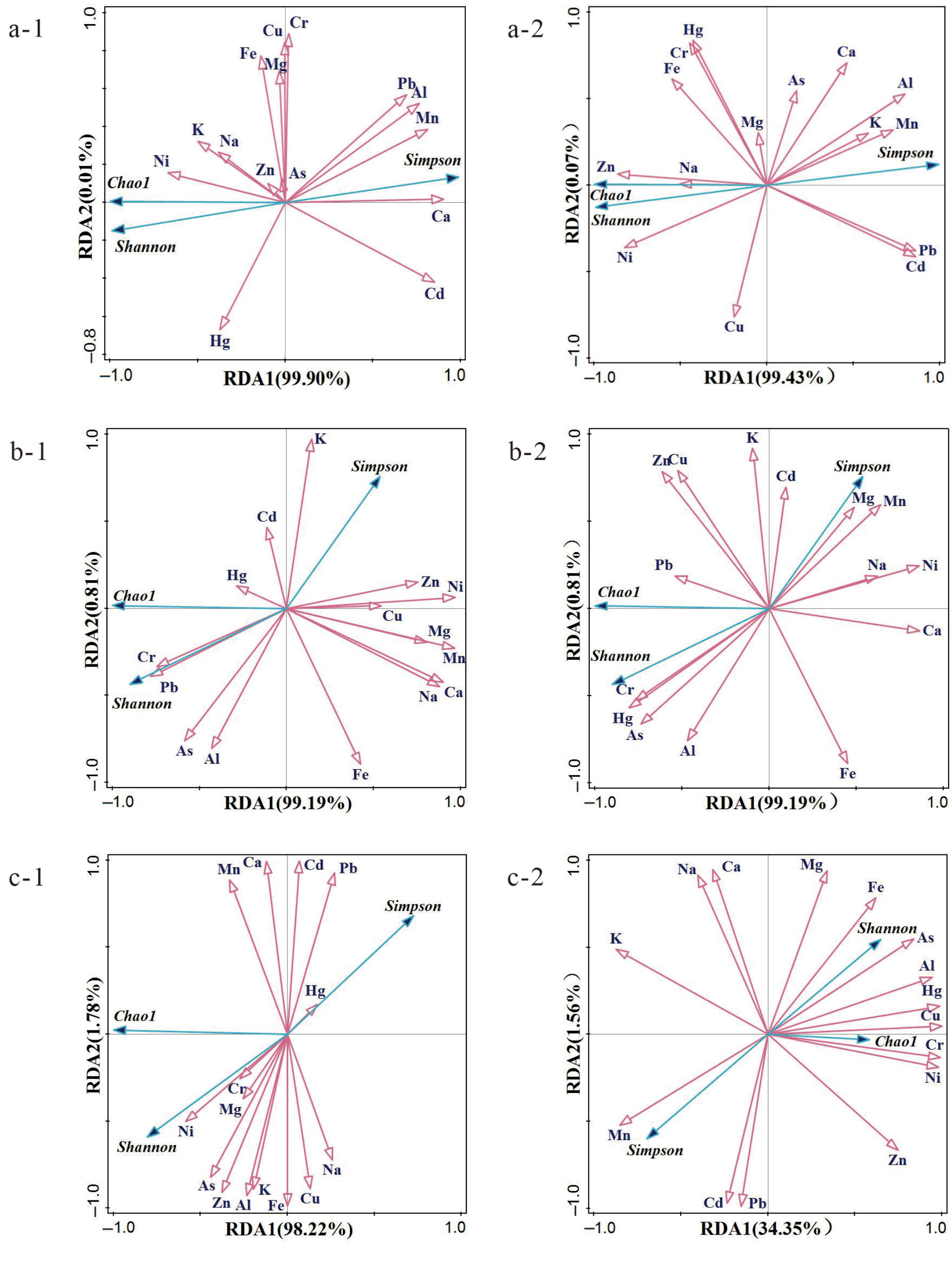

Figure 8. Exploratory redundancy analysis (RDA) of bioconcentration factors (BCF), tea leaf elements, and bacterial diversity across different lithologies: (**a**)-GT, (**b**)-QS, (**c**)-SS; **Left** panels display the exploratory redundancy analysis between BCF values and bacterial diversity, while **right** panels show the redundancy analysis between tea elements and bacterial diversity.

According to enrichment factor (EF) and bioconcentration factor (BCF) analyses (Table 6), K, Ca, and Mn were primarily enriched in tea leaves, Hg and Zn were mainly enriched in soils, while Cu and Cd were leached from soils and showed no enrichment in tea leaves. These elements were therefore selected for exploratory CART modeling. In the exploratory CART model (see Supplementary Material), nodes incorporated statistical parameters such as EF mean values, standard deviations, and sample sizes of K, Ca, Mn, Hg, Zn, Cu, and Cd, with splitting rules determined by potential predictor variables including clay minerals (e.g., illite, kaolinite, montmorillonite, chlorite), the chemical index of alteration, soil pH, and the relative abundances of bacterial phyla (Acidobacteria, Proteobacteria, Chloroflexi, Nitrospirae, Gemmatimonadetes, Actinobacteria, Bacteroidetes, Armatimonadetes, candidate division WPS-1, Verrucomicrobia, and Planctomycetes). The exploratory CART results suggested that soil elemental concentrations were the primary candidate splitting variables associated with the translocation of K, Ca, Cu, Zn, and Hg. Among these, Ca exhibited the highest EF mean, following the trend Ca > K > Cu > Zn > Hg, suggesting that Ca and K are more readily enriched in soils. While the exploratory model yielded high initial mathematical fits (e.g., $R^2 > 0.99$ for K, Ca, Cu, and Zn; $R^2 = 0.83$ for Hg). These values must be interpreted with extreme caution. Given the small sample size, these metrics reflect the organization of the current limited dataset rather than robust predictive relationships. The stability of these splits under resampling remains to be tested, and they serve purely to highlight patterns for future validation. As major elements, Ca and K are central to nutrient cycling, whereas trace elements can significantly alter their bioavailability [214]. This is consistent with the correlation heatmap (Figure 3c), which showed significant negative correlations between Ca and Cu, and between K and Hg. Elemental translocation and plant uptake efficiency are strongly associated with their bioavailable concentrations in the soil, which are in turn influenced by total concentrations, mineral interactions, microbial activity, and soil pH [215]. Kaolinite emerged as the initial candidate splitting variable for Mn translocation, with an apparent high model fit ($R^2 = 0.99$) that merits external testing. Mineral-element correlation analysis revealed a strong positive association between kaolinite and Mn (Figure 6a). Previous studies demonstrate that kaolinite surfaces can oxidize Mn(II) and promote the crystallization of Mn oxides such as hausmannite and manganite [216]. For Cd, the primary splitting variable was Armatimonadetes, with chlorite showing the highest contribution to the exploratory model ($R^2 = 0.93$). At corresponding nodes, Acidobacteria was identified as a potential splitting factor for Mn, Proteobacteria for Cu, and Bacteroidetes for Hg. Correlation analyses (Figure 5a,b) further confirmed that Cd, Mn, and Hg were negatively associated with Armatimonadetes, Acidobacteria, and Bacteroidetes.

Microbial processes such as bacterial cell surface adsorption, biomineralization, and biotransformation are known to affect elemental migration and enrichment. Functional groups on bacterial cell surfaces mediate electrostatic adsorption and complexation with metal ions, while microbial redox reactions can alter ionic valence states, inducing the precipitation of insoluble minerals and thereby reducing metal mobility and bioavailability [217,218]. For instance, microbial activity can interfere with Mn translocation pathways [219]. Extracellular polymeric substances (EPS) secreted by bacteria further influence the migration, transformation, distribution, and diffusion of both trace elements and major elements. Specifically, Proteobacteria can reduce soluble Cu(II) to insoluble Cu(I), promoting copper biomineralization and reducing its ecological toxicity [220,221]. Similarly, Hg contamination strongly shapes the relative abundance of Bacteroidetes, which in turn can regulate Hg migration and accumulation through their metabolic activity [222].

In the exploratory CART model, illite was identified as the splitting variable potentially associated with the migration of K, Ca, and Zn, which is consistent with the strong positive correlations observed in the heatmap (Figure 7a). The migration of K, Ca, and Zn is closely linked to the formation and transformation of illite, which can alter the distribution and mobility of these elements in soils through mechanisms such as adsorption and ion exchange [223,224]. At the same decision nodes, Planctomycetes acted as the candidate splitting factor for K and Zn migration, whereas Proteobacteria served as the candidate splitting factor for Ca migration.

Planctomycetes possess unique ecological and metabolic capacities, enabling them to degrade complex organic matter and release soluble K, thereby potentially influencing elemental mobility and enrichment. In parallel, their decomposition activities alter soil pH, which further modulates the solubility and migration of K and Zn [225]. Proteobacteria facilitate Ca migration by secreting organic acids that dissolve calcium carbonate, releasing Ca^{2+} ions into the soil [226]. Furthermore, Ca can mediate physicochemical interactions between organic compounds and minerals, enhancing the deposition of microbial cells and plant decomposition products on mineral surfaces, which can substantially reshape bacterial community structure in acidic soils [227,228]. Exploratory CART analysis also identified soil pH as a splitting factor at similar nodes involving K, Ca, Mn, and Cu migration. Soil pH is a widely recognized factor associated with nutrient availability for tea growth, with acidic soils significantly reducing the bioavailability of major elements such as K and Ca [229]. Moreover, pH is a critical driver of trace element mobility and bioavailability. Variations in soil pH alter the solubility, adsorption capacity, and migration of trace elements. In acidic conditions, trace element solubility increases, thereby enhancing their mobility [214].

CART serves as a useful heuristic framework to highlight candidate correlations between soil elemental EF values and both numerical and non-numerical variables [11]. Based on the exploratory CART modeling, we analyzed the complex relationships among bacterial communities, clay minerals, pH, and elemental migration-enrichment. The analysis suggested that soil concentrations of K, Ca, Cu, Zn, and Hg were the primary candidate factors associated with their migration, kaolinite was the initial splitting factor for Mn migration, and Armatimonadetes was the candidate splitting factor for Cd migration. Overall, soil functions as a complex ecological system in which clay minerals modulate elemental migration and enrichment through adsorption, precipitation, and ion-exchange processes, while bacteria directly or indirectly influence elemental mobility via extracellular precipitation, intracellular accumulation, and redox transformations.

5. Conclusions

The lithology of parent rocks strongly influences the elemental distribution and mineralogical characteristics of tea plantation soils. Through pedogenic weathering, these geological variations are closely associated with the composition, structure, and potential functions of soil bacterial communities, ultimately showing potential associations with the bioavailability, root uptake, and translocation of elements within the rock–soil–tea continuum.

The geochemical profiles of these soils are closely associated with their underlying bedrock. Specifically, granite-derived soils (dominated by feldspar weathering) are enriched in major nutrients (K, Na, Ca, Mg) and exhibit the highest overall bacterial diversity. Quartz schist soils, associated with quartz and chlorite, significantly accumulate transition metals and trace elements (Fe, Mn, Cu, Zn, Pb, Cr). Sericite schist soils are characterized by advanced secondary clay minerals (montmorillonite and kaolinite). Although Acidobacteria, Proteobacteria, and Chloroflexi remain universally dominant phyla across all sites, exploratory statistical evaluations reveal that elevated trace elements (e.g., Hg, Cr, Pb, Zn, As) potentially antagonize the uptake of essential major elements (Ca, Mg, Na) through competitive interactions. Rather than exhibiting uniform networks, bacterial proliferation is differentially associated with local chemical weathering intensity (CIA, CIW, WIP), pH fluctuations, and specific elemental stressors.

Exploratory assessments suggested a potential positive feedback coupling between bacterial communities and mineral weathering during pedogenesis, which relatively enriches elements like Hg, Pb, Al, and Mn. Correlation analyses demonstrated distinct, lithology-dependent "microbial–mineral–element" interactions within this dataset. In granite soils, chlorite was significantly associated with the migration of Cr, Pb, and Cu, potentially altering the relative abundances of Verrucomicrobia and Chloroflexi. In quartz schist, kaolinite statistically correlated with Pb and As mobility, potentially impacting Proteobacteria. In sericite schist, clay minerals (e.g., illite, limonite) exhibited the strongest statistical coupling with elemental migration (Pb, K, Ca), predominantly associating with Planctomycetes diversity.

During the soil-to-tea transfer stage, the elemental accumulation capacity generally follows the order: Ca > K > Mn > Mg > Na > Al. Spearman correlation networks revealed distinct, lithology-specific relationships; for instance, the soil bacterial Shannon index exhibited opposite correlations with K bioconcentration factors (BCF) between granite/sericite schist (positive) and quartz schist (negative). Furthermore, exploratory decision-tree analyses (detailed in the Supplementary Material) provided preliminary statistical support for potential elemental migration correlates. CART analysis suggested that while the migration of K, Ca, Cu, Zn, and Hg was primarily associated with their absolute soil concentrations, Mn migration was strongly linked to mineralogy (kaolinite content). Notably, Cd mobility was statistically correlated with the relative abundance of Armatimonadetes, underscoring candidate relationships between bacterial communities and elemental translocation.

Overall, by employing an exploratory statistical framework, this study highlights the potential interactive effects among bedrock lithology, elemental cycling, and soil bacterial communities. Crucially, this study identifies lithology-specific patterns and associations, not causal mechanisms. These findings are hypothesis-generating and require validation in larger or experimental datasets. These findings provide data-driven insights into utilizing bacteria–element interactions to potentially improve soil health and tea quality. Future research integrating broader environmental drivers and larger sample cohorts will be essential to further validate and refine these candidate models.

Supplementary Materials: The following supporting information can be downloaded at: https://www.mdpi.com/article/10.3390/min16030333/s1, Figure S1: Exploratory decision tree model utilizing the Classification and Regression Tree (CART) method to evaluate potential candidate predictors of the enrichment factor (EF) in soil element migration. (a–g) Decision tree structures for K, Ca, Mn, Zn, Cu, Cd, and Hg, respectively, based on soil geochemical properties and bacterial relative abundances. (a-1–g-1) Relative importance of independent variables for each model. (a-2–g-2) Scatter plots comparing actual versus predicted EF values. Note: Given the localized scale of the dataset (13 plantations), these CART models are utilized strictly as exploratory, hypothesis-generating tools rather than robust predictive frameworks. The high initial R^2 values reflect the mathematical organization of the current limited dataset. The specific splitting nodes should be interpreted as potential candidate associations awaiting future validation in larger or experimental datasets.

Author Contributions: R.L.: Writing—original draft, Visualization, H.C., Y.S.: Writing—review and editing, Methodology, P.P., L.Z., Y.H.: Investigation, H.B., J.G., S.L., J.C.: Validation, M.X., K.L., W.Z., W.Y.: Supervision. All authors have read and agreed to the published version of the manuscript.

Funding: This research was funded by the Department of Human Resources and Social Security of Yunnan Province through the "Yunnan Xingdian Talent Support Program" Youth Talent Project (no grant number issued).

Data Availability Statement: The data supporting the findings of this study are available within the article and its Supplementary Materials. Any additional datasets generated and/or analyzed during the current study are available from the corresponding author upon reasonable request.

Acknowledgments: The authors express their sincere gratitude to Yinxian Song of Kunming University of Science and Technology for his expert guidance in whole-rock and soil geochemistry. We are also deeply thankful to He Chang for his valuable insights regarding the relationship between soil bacterial communities and tea plant growth. Our appreciation further extends to all colleagues who provided assistance during the experimental phase of this study. Finally, we extend our sincere thanks to the editors and anonymous reviewers for their constructive feedback, which has substantially enhanced the academic quality of this manuscript.

Conflicts of Interest: The authors declare no conflicts of interest. The funders had no role in the design of the study; in the collection, analyses, or interpretation of data; in the writing of the manuscript; or in the decision to publish the results.

Abbreviations

The following abbreviations are used in this manuscript:

CIA	Chemical Index of Alteration
CIW	Chemical Index of Weathering
WIP	Weathering Index of Parker
EF	Enrichment Factor
BCF	Bioconcentration Factor

References

1. Pan, S.-Y.; Nie, Q.; Tai, H.-C.; Song, X.-L.; Tong, Y.-F.; Zhang, L.-J.-F.; Wu, X.-W.; Lin, Z.-H.; Zhang, Y.-Y.; Ye, D.-Y.; et al. Tea and Tea Drinking: China's Outstanding Contributions to the Mankind. *Chin. Med.* **2022**, *17*, 27. [CrossRef]
2. Hasimoto, M. The Origin of the Tea Plant. In Proceedings of the 2001 International Conference on O–Cha (Tea) Culture and Science (Session II), Shizuoka, Japan, 5–8 October 2001.
3. Trevisanato, S.I.; Kim, Y.I. Tea and Health. *Nutr. Rev.* **2000**, *58*, 1–10. [CrossRef]
4. Jia, M.; Wang, Y.; Zhang, Q.; Lin, S.; Zhang, Q.; Chen, Y.; Hong, L.; Jia, X.; Ye, J.; Wang, H. Effect of Soil pH on the Uptake of Essential Elements by Tea Plant and Subsequent Impact on Growth and Leaf Quality. *Agronomy* **2024**, *14*, 1338. [CrossRef]
5. Zhao, Y.; Li, L.; Ma, S.; Han, R.; He, Y.; Zhu, J.; Li, M.; Zhuang, J.; Wang, Y.; Zhao, Z. Mn-CDF Family Genes Enhance the Manganese Tolerance of the Tea Plants (*Camellia sinensis*) under Acidic Condition. *Plant Physiol. Biochem.* **2024**, *216*, 109179. [CrossRef] [PubMed]
6. Wang, H.; Yuan, W.; Wang, Q.; Xia, Y.; Chun, W.; Li, H.; Peng, G.; Huang, W.; Wang, B. Comprehensive Assessment of the Correlation between Ancient Tea Garden Soil Chemical Properties and Tea Quality. *Horticulturae* **2024**, *10*, 1207. [CrossRef]
7. Wang, D.; Liu, B.; Li, F.; Wang, Z.; Hou, J.; Cao, R.; Zheng, Y.; Yang, W. Status and Influential Factors of Soil Nutrients and Acidification in Chinese Tea Plantations: A Meta-Analysis. *Soil* **2025**, *11*, 175–191. [CrossRef]
8. Zhang, H.; Song, Y.; Fan, Z.; Ruan, J.; Hu, J.; Zhang, Q. Aluminum Supplementation Mediates the Changes in Tea Plant Growth and Metabolism in Response to Calcium Stress. *Int. J. Mol. Sci.* **2023**, *25*, 530. [CrossRef]
9. Hao, J.; Peng, A.; Li, Y.; Zuo, H.; Li, P.; Wang, J.; Yu, K.; Liu, C.; Zhao, S.; Wan, X.; et al. Tea Plant Roots Respond to Aluminum-Induced Mineral Nutrient Imbalances by Transcriptional Regulation of Multiple Cation and Anion Transporters. *BMC Plant Biol.* **2022**, *22*, 203. [CrossRef]
10. Cong, Y.; Yu, R.; Yan, Y.; Weng, B.; Hu, G.; Sun, J.; Cui, J.; Huang, Y. Source Analysis of Metals in the Tea Plant Using Linear Correlation Analysis Combined with a Lead-Strontium Isotope Tracer. *Catena* **2023**, *229*, 107194. [CrossRef]
11. Tao, C.; Song, Y.; Chen, Z.; Zhao, W.; Ji, J.; Shen, N.; Ayoko, G.A.; Frost, R.L. Geological Load and Health Risk of Heavy Metals Uptake by Tea from Soil: What Are the Significant Influencing Factors? *Catena* **2021**, *204*, 105419. [CrossRef]
12. Zhan, Y.; Zhu, Q.; Li, X.; Tao, C.; Su, H.; Wu, Y.; Lin, J.; Zhang, Y.; Huang, Y.; Jiang, F. The Distribution Characteristics and Potential Risk Assessment of Lead in the Soil of Tieguanyin Tea Plantations in Anxi County, China. *Toxics* **2023**, *12*, 22. [CrossRef]
13. Zhang, J.; Yang, R.; Li, Y.C.; Peng, Y.; Wen, X.; Ni, X. Distribution, Accumulation, and Potential Risks of Heavy Metals in Soil and Tea Leaves from Geologically Different Plantations. *Ecotoxicol. Environ. Saf.* **2020**, *195*, 110475. [CrossRef] [PubMed]
14. Karak, T.; Abollino, O.; Bhattacharyya, P.; Das, K.K.; Paul, R.K. Fractionation and Speciation of Arsenic in Three Tea Gardens Soil Profiles and Distribution of As in Different Parts of Tea Plant (*Camellia sinensis* L.). *Chemosphere* **2011**, *85*, 948–960. [CrossRef] [PubMed]
15. Lin, S.; Liu, X.; Yan, Q.; Liang, G.; Wang, D. Research on Heavy Metal Enrichment and Transportation in Tea Plant-Soil Systems of Different Varieties. *Environ. Geochem. Health* **2024**, *46*, 514. [CrossRef] [PubMed]
16. de Oliveira, L.M.; Das, S.; da Silva, E.B.; Gao, P.; Gress, J.; Liu, Y.; Ma, L.Q. Metal Concentrations in Traditional and Herbal Teas and Their Potential Risks to Human Health. *Sci. Total Environ.* **2018**, *633*, 649–657. [CrossRef]
17. Shaheen, N.; Irfan, N.M.; Khan, I.N.; Islam, S.; Islam, M.S.; Ahmed, M.K. Presence of Heavy Metals in Fruits and Vegetables: Health Risk Implications in Bangladesh. *Chemosphere* **2016**, *152*, 431–438. [CrossRef]

18. Nadeem, F.; Abbas, S.; Waseem, F.; Ali, N.; Mahmood, R.; Bibi, S.; Deng, L.; Wang, R.; Zhong, Y.; Li, X. Phosphorus (P) and Zinc (Zn) Nutrition Constraints: A Perspective of Linking Soil Application with Plant Regulations. *Environ. Exp. Bot.* **2024**, *226*, 105875. [CrossRef]
19. Huang, X.; Zheng, Y.; Li, P.; Cui, J.; Sui, P.; Chen, Y.; Gao, W. Organic Management Increases Beneficial Microorganisms and Promotes the Stability of Microecological Networks in Tea Plantation Soil. *Front. Microbiol.* **2023**, *14*, 1237842. [CrossRef]
20. Lin, S.; Liu, Z.; Wang, Y.; Li, J.; Wang, G.; Ye, J.; Wang, H.; He, H. Soil Metagenomic Analysis on Changes of Functional Genes and Microorganisms Involved in Nitrogen-Cycle Processes of Acidified Tea Soils. *Front. Plant Sci.* **2022**, *13*, 998178. [CrossRef]
21. Yang, Y.; Kim, J.; Chung, J.-O.; Cho, D.; Roh, J.-H.; Hong, Y.-D.; Kim, W.-G.; Kang, H. Variations in the Composition of Tea Leaves and Soil Microbial Community. *Biol. Fertil. Soils* **2022**, *58*, 167–179. [CrossRef]
22. Zhao, Y.; Zhang, N.; Chen, J.; Ran, W.; Zhao, Z.; Song, Y. Interpretation of Bacterial Composition Patterns and Community Assembly Processes in the Rhizosphere Soil of Tea Trees in Karst Areas. *BMC Microbiol.* **2024**, *24*, 492. [CrossRef]
23. Jibola-Shittu, M.Y.; Heng, Z.; Keyhani, N.O.; Dang, Y.; Chen, R.; Liu, S.; Lin, Y.; Lai, P.; Chen, J.; Yang, C. Understanding and Exploring the Diversity of Soil Microorganisms in Tea (Camellia Sinensis) Gardens: Toward Sustainable Tea Production. *Front. Microbiol.* **2024**, *15*, 1379879. [CrossRef] [PubMed]
24. Wang, M.; Sun, H.; Xu, L.; Xu, Z. Bacterial Diversity in Tea Plant (*Camellia sinensis*) Rhizosphere Soil from Qinling Mountains and Its Relationship with Environmental Elements. *Plant Soil* **2021**, *460*, 403–415. [CrossRef]
25. Bora, S.S.; Hazarika, D.J.; Gogoi, R.; Dullah, S.; Gogoi, M.; Barooah, M. Long-Term Pruning Modulates Microbial Community Structure and Their Functional Potential in Tea (*Camellia sinensis* L.) Soils. *Appl. Soil Ecol.* **2022**, *176*, 104483. [CrossRef]
26. Gui, H.; Fan, L.; Wang, D.; Yan, P.; Li, X.; Pang, Y.; Zhang, L.; Zamanian, K.; Shi, L.; Xu, J. Variations in Soil Nutrient Dynamics and Bacterial Communities after the Conversion of Forests to Long-Term Tea Monoculture Systems. *Front. Microbiol.* **2022**, *13*, 896530. [CrossRef] [PubMed]
27. Wei, S.; Liu, B.; Ni, K.; Ma, L.; Shi, Y.; Leng, Y.; Zheng, S.; Gao, S.; Yang, X.; Ruan, J. Rhizosphere Microbial Community Shows a Greater Response than Soil Properties to Tea (*Camellia sinensis* L.) Cultivars. *Agronomy* **2023**, *13*, 221. [CrossRef]
28. Pu, T.; Zhang, N.; Wang, J.; Zhao, Z.; Tan, W.; Li, C.; Song, Y. Organic Management Pattern Improves Microbial Community Diversity and Alters Microbial Network Structure in Karst Tea Plantation. *Heliyon* **2024**, *10*, e31528. [CrossRef]
29. Yan, Y.; Zhou, D.; Yang, Y.; Xie, J.; Lü, C.; Yang, G.; Wen, Q. Influence of Organic Planting on Soil Microbial Community Composition and Diversity in Tea Gardens. *J. Tea Sci.* **2024**, *44*, 264.
30. Shao, S.; Li, Y.; Li, Z.; Ma, X.; Zhu, Y.; Luo, Y.; Cai, P.; Jia, X.; Rensing, C.; Li, Q. Impact of Tea Tree Cultivation on Soil Microbiota, Soil Organic Matter, and Nitrogen Cycling in Mountainous Plantations. *Agronomy* **2024**, *14*, 638. [CrossRef]
31. Chen, W.-C.; Ko, C.-H.; Su, Y.-S.; Lai, W.-A.; Shen, F.-T. Metabolic Potential and Community Structure of Bacteria in an Organic Tea Plantation. *Appl. Soil Ecol.* **2021**, *157*, 103762. [CrossRef]
32. Guo, H.; Chen, L.; Wang, Y.; Li, Q.; Yi, Z. Combined Application of Biochar and Magnesium Fertilizer Effectively Improved the Soil Environment and the Tea Quality in Southern Strongly Acidic Tea Garden. *J. Soils Sediments* **2023**, *23*, 2798–2815. [CrossRef]
33. Yang, W.; Ji, Z.; Wu, A.; He, D.; Rensing, C.; Chen, Y.; Chen, C.; Wu, H.; Muneer, M.A.; Wu, L. Inconsistent Responses of Soil Bacterial and Fungal Community's Diversity and Network to Magnesium Fertilization in Tea (*Camellia sinensis*) Plantation Soils. *Appl. Soil Ecol.* **2023**, *191*, 105055. [CrossRef]
34. Zhang, S.; Yanagisawa, N.; Asahina, M.; Yamashita, H.; Ikka, T. Soil Chemical Factors Contributing to Differences in Bacterial Communities among Tea Field Soils and Their Relationships with Tea Quality. *Front. Plant Sci.* **2025**, *16*, 1540659. [CrossRef] [PubMed]
35. Meena, V.S.; Maurya, B.R.; Verma, J.P.; Meena, R.S. (Eds.) *Potassium Solubilizing Microorganisms for Sustainable Agriculture*; Springer: New Delhi, India, 2016.
36. Yadav, B.K.; Sidhu, A.S. Dynamics of Potassium and Their Bioavailability for Plant Nutrition. In *Potassium Solubilizing Microorganisms for Sustainable Agriculture*; Meena, V.S., Maurya, B.R., Verma, J.P., Meena, R.S., Eds.; Springer: New Delhi, India, 2016; pp. 187–201.
37. Singh, A.K.; Pathak, S.K. Potassium in Tea (*Camellia sinensis* (L) O. Kuntze) Cultivation from Soil to Cup Quality—A Review. *Agric. Rev.* **2018**, *39*, 40–47. [CrossRef]
38. Dong, H.; Huang, L.; Zhao, L.; Zeng, Q.; Liu, X.; Sheng, Y.; Shi, L.; Wu, G.; Jiang, H.; Li, F. A Critical Review of Mineral–Microbe Interaction and Co-Evolution: Mechanisms and Applications. *Natl. Sci. Rev.* **2022**, *9*, nwac128. [CrossRef]
39. Gataraddi, S.; Aladakatti, R.H.; Patil, S.J.; Sadashiv, S.O. Microbe–Mineral Interactions: Environmental Pollution and Management. In *Biotechnology for Environmental Sustainability*; Verma, P., Ed.; Interdisciplinary Biotechnological Advances; Springer Nature: Singapore, 2025; pp. 661–671.
40. Etesami, H. Bacterial Mediated Alleviation of Heavy Metal Stress and Decreased Accumulation of Metals in Plant Tissues: Mechanisms and Future Prospects. *Ecotoxicol. Environ. Saf.* **2018**, *147*, 175–191. [CrossRef]
41. Zhang, Z.; Deng, Q.; Ye, H.; Ge, G. Bacterial and Fungal Diversities Examined through High-Throughput Sequencing in Response to Lead Contamination of Tea Garden Soil. *Front. Microbiol.* **2023**, *14*, 1121199. [CrossRef]

42. Huang, X.; Wang, X.; Wu, Q.; Zhang, Z.; Yang, H.; Wen, X. Effects of Multiple-Metal-Compound Contamination on the Soil Microbial Community in Typical Karst Tea Plantations. *Forests* **2023**, *14*, 1840. [CrossRef]
43. Song, L.; Niu, X.; Zhou, B.; Xiao, Y.; Zou, H. Application of Biochar-Immobilized Bacillus Sp. KSB7 to Enhance the Phytoremediation of PAHs and Heavy Metals in a Coking Plant. *Chemosphere* **2022**, *307*, 136084. [CrossRef]
44. Wang, C.; Huang, Y.; Yang, X.; Xue, W.; Zhang, X.; Zhang, Y.; Pang, J.; Liu, Y.; Liu, Z. Burkholderia Sp. Y4 Inhibits Cadmium Accumulation in Rice by Increasing Essential Nutrient Uptake and Preferentially Absorbing Cadmium. *Chemosphere* **2020**, *252*, 126603. [CrossRef]
45. González Henao, S.; Ghneim-Herrera, T. Heavy Metals in Soils and the Remediation Potential of Bacteria Associated with the Plant Microbiome. *Front. Environ. Sci.* **2021**, *9*, 604216. [CrossRef]
46. Geszvain, K.; McCarthy, J.K.; Tebo, B.M. Elimination of Manganese(II,III) Oxidation in Pseudomonas Putida GB-1 by a Double Knockout of Two Putative Multicopper Oxidase Genes. *Appl. Environ. Microbiol.* **2013**, *79*, 357–366. [CrossRef] [PubMed]
47. Bacteriogenic Manganese Oxides. Available online: https://pubs.acs.org/doi/abs/10.1021/ar800232a (accessed on 11 March 2026).
48. Dai, Z.; Guo, X.; Lin, J.; Wang, X.; He, D.; Zeng, R.; Meng, J.; Luo, J.; Delgado-Baquerizo, M.; Moreno-Jiménez, E. Metallic Micronutrients Are Associated with the Structure and Function of the Soil Microbiome. *Nat. Commun.* **2023**, *14*, 8456. [CrossRef] [PubMed]
49. Da Costa, C.; Colin, Y.; Debret, M.; Copard, Y.; Gardes, T.; Jacq, K.; Ayrault, S.; Berthe, T. Shifts in Sediment Bacterial Communities Reflect Changes in Depositional Environments in a Fluviatile Context. *Sci. Total Environ.* **2023**, *885*, 163890. [CrossRef] [PubMed]
50. Liu, Y.; Lu, M.; Zhang, X.; Sun, Q.; Liu, R.; Lian, B. Shift of the Microbial Communities from Exposed Sandstone Rocks to Forest Soils during Pedogenesis. *Int. Biodeterior. Biodegrad.* **2019**, *140*, 21–28. [CrossRef]
51. Li, F.; Jing, M.; Ma, F.; Wang, W.; Li, M. Comparison and Risk Assessment of Macroelements and Trace Metals in Commercial Teas from Different Regions of China. *Biol. Trace Elem. Res.* **2023**, *201*, 1503–1519. [CrossRef]
52. He, C.; Zhao, Y.; Zhang, H.; Wang, Z.; Lü, J.; Ge, L.; Zhao, X.; Xu, C. Detoxification Effect of Selenium: Alleviating the Inhibition of Cadmium Stress on the Growth of Rape (*Brassica Napus* L.) by Regulating Photosynthetic Pigments, Metal Complexation Reaction, and Antioxidant System. *Agronomy* **2025**, *15*, 541. [CrossRef]
53. Parker, A. An Index of Weathering for Silicate Rocks. *Geol. Mag.* **1970**, *107*, 501–504. [CrossRef]
54. Nesbitt, H.W.; Young, G.M. Prediction of Some Weathering Trends of Plutonic and Volcanic Rocks Based on Thermodynamic and Kinetic Considerations. *Geochim. Cosmochim. Acta* **1984**, *48*, 1523–1534. [CrossRef]
55. Harnois, L. The CIW Index: A New Chemical Index of Weathering. *Sediment. Geol.* **1988**, *55*, 319–322. [CrossRef]
56. Müller, G. Index of Geoaccumulation in Sediments of the Rhine River. *GeoJournal* **1969**, *2*, 108–118.
57. Krauskopf, K.B.; Bird, D.K. *Introduction to Geochemistry*; McGraw-Hill: New York, NY, USA, 1995; Volume 647.
58. McLennan, S.M. Weathering and Global Denudation. *J. Geol.* **1993**, *101*, 295–303. [CrossRef]
59. Anda, M. Cation Imbalance and Heavy Metal Content of Seven Indonesian Soils as Affected by Elemental Compositions of Parent Rocks. *Geoderma* **2012**, *189*, 388–396. [CrossRef]
60. Breiter, K.; Ďurišová, J.; Dosbaba, M. Chemical Signature of Quartz from S-and A-Type Rare-Metal Granites–A Summary. *Ore Geol. Rev.* **2020**, *125*, 103674. [CrossRef]
61. Astakhova, N.V.; Ivanov, V.V.; Aksentov, K.I. Petrogeochemistry and Ore Mineralization of Sericite–Quartz Schists of the Southern Slope of the Kashevarov Bank (Sea of Okhotsk). *Oceanology* **2021**, *61*, 701–713. [CrossRef]
62. Heinrichs, H.; Schulz-Dobrick, B.; Wedepohl, K.H. Terrestrial Geochemistry of Cd, Bi, Tl, Pb, Zn and Rb. *Geochim. Cosmochim. Acta* **1980**, *44*, 1519–1533. [CrossRef]
63. Addesso, R.; Araniti, F.; Bloise, A.; Mininni, A.N.; Dichio, B.; López-González, D.; Elshafie, H.S.; Ellerbrock, R.H.; Schnee, L.S.; Filser, J. Soil Organic Matter Quality in an Olive Orchard Differently Managed for 21 Years: Insights into Its Distribution through Soil Aggregates and Depth. *Agric. Ecosyst. Environ.* **2025**, *380*, 109388. [CrossRef]
64. Dhaliwal, S.S.; Naresh, R.K.; Mandal, A.; Singh, R.; Dhaliwal, M.K. Dynamics and Transformations of Micronutrients in Agricultural Soils as Influenced by Organic Matter Build-up: A Review. *Environ. Sustain. Indic.* **2019**, *1*, 100007. [CrossRef]
65. Szymański, W. Chemistry and Spectroscopic Properties of Surface Horizons of Arctic Soils under Different Types of Tundra Vegetation–A Case Study from the Fuglebergsletta Coastal Plain (SW Spitsbergen). *Catena* **2017**, *156*, 325–337. [CrossRef]
66. Chappell, A.; Webb, N.P.; Leys, J.F.; Waters, C.M.; Orgill, S.; Eyres, M.J. Minimising Soil Organic Carbon Erosion by Wind Is Critical for Land Degradation Neutrality. *Environ. Sci. Policy* **2019**, *93*, 43–52. [CrossRef]
67. Jien, S.-H.; Wang, C.-S. Effects of Biochar on Soil Properties and Erosion Potential in a Highly Weathered Soil. *Catena* **2013**, *110*, 225–233. [CrossRef]
68. Wang, W.; Feng, J.; Qui, M. Mineral Weathering and Element Migration in Granite Weathering Pits (Gnammas): A Case Study in Eastern China. *Minerals* **2022**, *13*, 70. [CrossRef]
69. Huang, T.-Y.; Teng, F.-Z.; Wang, Z.-Z.; He, Y.-S.; Liu, Z.-C.; Wu, F.-Y. Potassium Isotope Fractionation during Granitic Magmatic Differentiation: Mineral-Pair Perspectives. *Geochim. Cosmochim. Acta* **2023**, *343*, 196–211. [CrossRef]

70. Starr, M.; Lindroos, A.-J. Changes in the Rate of Release of Ca and Mg and Normative Mineralogy Due to Weathering along a 5300-Year Chronosequence of Boreal Forest Soils. *Geoderma* **2006**, *133*, 269–280. [CrossRef]
71. Tebo, B.M.; Johnson, H.A.; McCarthy, J.K.; Templeton, A.S. Geomicrobiology of Manganese (II) Oxidation. *Trends Microbiol.* **2005**, *13*, 421–428. [CrossRef] [PubMed]
72. Rengel, Z. Availability of Mn, Zn and Fe in the Rhizosphere. *J. Soil Sci. Plant Nutr.* **2015**, *15*, 397–409. [CrossRef]
73. Arnfalk, P.; Wasay, S.A.; Tokunaga, S. A Comparative Study of Cd, Cr(III), Cr(VI), Hg, and Pb Uptake by Minerals and Soil Materials. *Water. Air. Soil Pollut.* **1996**, *87*, 131–148. [CrossRef]
74. Moreno-Jiménez, E.; Esteban, E.; Peñalosa, J.M. The Fate of Arsenic in Soil-Plant Systems. In *Reviews of Environmental Contamination and Toxicology*; Whitacre, D.M., Ed.; Springer: New York, NY, USA, 2012; Volume 215, pp. 1–37.
75. Tessema, D.A.; Mogessie, A.; Kosmus, W. Arsenopyrite Weathering and Leaching of Arsenic in an Austrian Soil. *Soil Sediment Contam. Int. J.* **2011**, *20*, 550–563. [CrossRef]
76. Vaxevanidou, K.; Giannikou, S.; Papassiopi, N. Microbial Arsenic Reduction in Polluted and Unpolluted Soils from Attica, Greece. *J. Hazard. Mater.* **2012**, *241*, 307–315. [CrossRef]
77. Yaroshevsky, A.A. Abundances of Chemical Elements in the Earth's Crust. *Geochem. Int.* **2006**, *44*, 48–55. [CrossRef]
78. Fan, B.; Yang, X.; Jiang, K.; Zhao, Z. Processes Controlling the Mg Isotope Behavior during Granite Weathering. *J. Asian Earth Sci.* **2023**, *251*, 105674. [CrossRef]
79. Jackson, T.A. Weathering, Secondary Mineral Genesis, and Soil Formation Caused by Lichens and Mosses Growing on Granitic Gneiss in a Boreal Forest Environment. *Geoderma* **2015**, *251*, 78–91. [CrossRef]
80. Beckers, F.; Rinklebe, J. Cycling of Mercury in the Environment: Sources, Fate, and Human Health Implications: A Review. *Crit. Rev. Environ. Sci. Technol.* **2017**, *47*, 693–794. [CrossRef]
81. Deng, D.; Wu, Y.; Sun, Y.; Ren, B.; Song, L. Pollution Characteristics and Spatial Distribution of Heavy Metals in Coal-Bearing Sandstone Soil: A Case Study of Coal Mine Area in Southwest China. *Int. J. Environ. Res. Public Health* **2022**, *19*, 6493. [CrossRef]
82. Tang, Z.; Zhang, X.; Zhang, M.; Zhou, M.; Tian, F.; Wang, S.; Ma, Q.; Wang, C.; Zhang, J.; Niu, X.; et al. Geochemical Characteristics of Soil Elements in Xin'an River Basin: Constraints from Rock Formation Types. *East China Geol.* **2023**, *44*, 172–185.
83. Woodruff, L.G.; Cannon, W.F.; Eberl, D.D.; Smith, D.B.; Kilburn, J.E.; Horton, J.D.; Garrett, R.G.; Klassen, R.A. Continental-Scale Patterns in Soil Geochemistry and Mineralogy: Results from Two Transects across the United States and Canada. *Appl. Geochem.* **2009**, *24*, 1369–1381. [CrossRef]
84. Zhao, T.; Xu, S.; Hao, F. Differential Adsorption of Clay Minerals: Implications for Organic Matter Enrichment. *Earth-Sci. Rev.* **2023**, *246*, 104598. [CrossRef]
85. Gougazeh, M.; Bamousa, A.; Hasan, A. Evaluation of Granitic Rocks as Feldspar Source: Al Madinah, Western Part of Saudi Arabia. *J. Taibah Univ. Sci.* **2018**, *12*, 21–36. [CrossRef]
86. Onwualu-John, J.N.; Nwosu, J.I. Mineralogical Description of Granitic Rocks at Auchi-Igarra and Okene-Lokoja Area, Nigeria. *Int. J. Innov. Environ. Stud. Res.* **2023**, *11*, 20–24.
87. Belaidi, H.; Kitouni, S.; Chellat, S. Evaluation of Some Granitic Rocks of the Algerian Coast as a Source of Feldspar Raw Material. *Period. Mineral.* **2024**, *93*, 35–50.
88. Garate-Olave, I.; Roda-Robles, E.; Gil-Crespo, P.P.; Pesquera, A. Mica and Feldspar as Indicators of the Evolution of a Highly Evolved Granite-Pegmatite System in the Tres Arroyos Area (Central Iberian Zone, Spain). *J. Iber. Geol.* **2018**, *44*, 375–403. [CrossRef]
89. Götze, J.; Pan, Y.; Müller, A. Mineralogy and Mineral Chemistry of Quartz: A Review. *Mineral. Mag.* **2021**, *85*, 639–664. [CrossRef]
90. Shah, S.A.; Shao, Y.; Zhang, Y.; Zhao, H.; Zhao, L. Texture and Trace Element Geochemistry of Quartz: A Review. *Minerals* **2022**, *12*, 1042. [CrossRef]
91. Deyell, C.L.; Thompson, J.F.; Friedman, R.M.; Groat, L.A. Age and Origin of Advanced Argillic Alteration Zones and Related Exotic Limonite Deposits in the Limonite Creek Area, Central British Columbia. *Can. J. Earth Sci.* **2000**, *37*, 1093–1107. [CrossRef]
92. Wu, F.; Cao, Z.; Wang, S.; Zhong, H. Novel and Green Metallurgical Technique of Comprehensive Utilization of Refractory Limonite Ores. *J. Clean. Prod.* **2018**, *171*, 831–843. [CrossRef]
93. Yang, J.; Xu, S.; Zhu, P.; Ma, S. Study on Process Mineralogy of Limonite. *J. Phys. Conf. Ser.* **2021**, *2133*, 012023. [CrossRef]
94. Zhao, D.; Ma, B.; Shi, B.; Zhou, Z.; Xing, P.; Wang, C. Mineralogical Characterization of Limonitic Laterite from Africa and Its Proposed Processing Route. *J. Sustain. Metall.* **2020**, *6*, 491–503. [CrossRef]
95. Shirozu, H. Chlorite Minerals. In *Developments in Sedimentology*; Elsevier: Amsterdam, The Netherlands, 1978; Volume 26, pp. 243–264.
96. Meunier, A.; Velde, B. Dynamics of the Smectite-to-Illite Transformation. In *Illite*; Springer: Berlin/Heidelberg, Germany, 2004; pp. 145–187.
97. Singh, B.; Schulze, D.G. Soil Minerals and Plant Nutrition. *Nat. Educ. Knowl.* **2015**, *6*, 1.
98. Yao, Z.; Zhang, H.; Zhang, H.; Wei, Y.; Niu, Y. Enrichment and Sources of Major and Trace Elements in the Qinghai-Tibetan Plateau: A Case Study of the Golog Prefecture. *Environ. Monit. Assess.* **2024**, *197*, 1. [CrossRef]

99. Bhattacharyya, K.G.; Gupta, S.S. Adsorption of a Few Heavy Metals on Natural and Modified Kaolinite and Montmorillonite: A Review. *Adv. Colloid Interface Sci.* **2008**, *140*, 114–131. [CrossRef]
100. Gupta, S.S.; Bhattacharyya, K.G. Adsorption of Heavy Metals on Kaolinite and Montmorillonite: A Review. *Phys. Chem. Chem. Phys.* **2012**, *14*, 6698–6723. [CrossRef] [PubMed]
101. Qiao, H.; Liu, Z.; Peng, X.; Xian, H.; Cheng, K.; Yang, F. Significance of Humic Matters-Soil Mineral Interactions for Environmental Remediation: A Review. *Chemosphere* **2024**, *365*, 143356. [CrossRef] [PubMed]
102. Acosta, J.A.; Martínez-Martínez, S.; Faz, A.; Arocena, J. Accumulations of Major and Trace Elements in Particle Size Fractions of Soils on Eight Different Parent Materials. *Geoderma* **2011**, *161*, 30–42. [CrossRef]
103. Hower, J.; Eslinger, E.V.; Hower, M.E.; Perry, E.A. Mechanism of Burial Metamorphism of Argillaceous Sediment: 1. Mineralogical and Chemical Evidence. *Geol. Soc. Am. Bull.* **1976**, *87*, 725–737. [CrossRef]
104. Liu, Z.; Tan, X.; Wang, J.; Ran, T.; Shen, J.; Xu, X.; Jiang, F. Formation Mechanism and Alteration of Clay Minerals in Clastic Rocks. *Adv. Geosci.* **2015**, *5*, 467–479. [CrossRef]
105. Zeng, X.; Cai, J.; Dong, Z.; Bian, L.; Li, Y. Relationship between Mineral and Organic Matter in Shales: The Case of Shahejie Formation, Dongying Sag, China. *Minerals* **2018**, *8*, 222. [CrossRef]
106. Finley, B.K.; Mau, R.L.; Hayer, M.; Stone, B.W.; Morrissey, E.M.; Koch, B.J.; Rasmussen, C.; Dijkstra, P.; Schwartz, E.; Hungate, B.A. Soil Minerals Affect Taxon-Specific Bacterial Growth. *ISME J.* **2022**, *16*, 1318–1326. [CrossRef]
107. Lei, Y.; Ding, D.; Duan, J.; Luo, Y.; Huang, F.; Kang, Y.; Chen, Y.; Li, S. Soil Microbial Community Characteristics and Their Effect on Tea Quality under Different Fertilization Treatments in Two Tea Plantations. *Genes* **2024**, *15*, 610. [CrossRef]
108. Lin, Y.-T.; Lin, Y.-F.; Tsai, I.J.; Chang, E.-H.; Jien, S.-H.; Lin, Y.-J.; Chiu, C.-Y. Structure and Diversity of Soil Bacterial Communities in Offshore Islands. *Sci. Rep.* **2019**, *9*, 4689. [CrossRef]
109. Voutsinos, M.Y.; West-Roberts, J.A.; Sachdeva, R.; Moreau, J.W.; Banfield, J.F. Weathered Granites and Soils Harbour Microbes with Lanthanide-Dependent Methylotrophic Enzymes. *BMC Biol.* **2024**, *22*, 41. [CrossRef]
110. Choe, Y.-H.; Kim, M.; Woo, J.; Lee, M.J.; Lee, J.I.; Lee, E.J.; Lee, Y.K. Comparing Rock-Inhabiting Microbial Communities in Different Rock Types from a High Arctic Polar Desert. *FEMS Microbiol. Ecol.* **2018**, *94*, fiy070. [CrossRef]
111. Dlamini, P.; Sekhohola-Dlamini, L.M.; Cowan, A.K. Soil-Microbial Interactions. *Front. Microbiol.* **2023**, *14*, 1213834. [CrossRef] [PubMed]
112. Kielak, A.M.; Barreto, C.C.; Kowalchuk, G.A.; Van Veen, J.A.; Kuramae, E.E. The Ecology of Acidobacteria: Moving beyond Genes and Genomes. *Front. Microbiol.* **2016**, *7*, 744. [CrossRef] [PubMed]
113. Dedysh, S.N.; Sinninghe Damsté, J.S. Acidobacteria. In *Encyclopedia of Life Sciences*; Wiley: Hoboken, NJ, USA, 2018; pp. 1–10.
114. Zhang, Y.; Cong, J.; Lu, H.; Li, G.; Qu, Y.; Su, X.; Zhou, J.; Li, D. Community Structure and Elevational Diversity Patterns of Soil Acidobacteria. *J. Environ. Sci.* **2014**, *26*, 1717–1724. [CrossRef] [PubMed]
115. Wang, Y.; Osman, J.R.; DuBow, M.S. Bacterial Communities on the Surface of the Mineral Sandy Soil from the Desert of Maine (USA). *Curr. Microbiol.* **2020**, *77*, 1429–1437. [CrossRef]
116. Ablimit, R.; Li, W.; Zhang, J.; Gao, H.; Zhao, Y.; Cheng, M.; Meng, X.; An, L.; Chen, Y. Altering Microbial Community for Improving Soil Properties and Agricultural Sustainability during a 10-Year Maize-Green Manure Intercropping in Northwest China. *J. Environ. Manag.* **2022**, *321*, 115859. [CrossRef]
117. Zhang, H.; Gao, Z.; Shi, M.; Fang, S. Soil Bacterial Diversity and Its Relationship with Soil CO2 and Mineral Composition: A Case Study of the Laiwu Experimental Site. *Int. J. Environ. Res. Public Health* **2020**, *17*, 5699. [CrossRef]
118. Buckley, D.H.; Huangyutitham, V.; Nelson, T.A.; Rumberger, A.; Thies, J.E. Diversity of *Planctomycetes* in Soil in Relation to Soil History and Environmental Heterogeneity. *Appl. Environ. Microbiol.* **2006**, *72*, 4522–4531. [CrossRef]
119. Retamal-Morales, G.; Mehnert, M.; Schwabe, R.; Tischler, D.; Zapata, C.; Chávez, R.; Schlömann, M.; Levicán, G. Detection of Arsenic-Binding Siderophores in Arsenic-Tolerating Actinobacteria by a Modified CAS Assay. *Ecotoxicol. Environ. Saf.* **2018**, *157*, 176–181. [CrossRef]
120. Fuyun, G.A.O.; Yaying, L.I.; Haoxin, F.A.N.; Jiantao, X.U.E.; Huaiying, Y.A.O. Main Environmental Drivers of Abundance, Diversity and Community Structure of Comammox Nitrospira in Paddy Soils. *Pedosphere* **2023**, *33*, 808–818.
121. Keyhani, A.B.; He, W.; Teng, M.; Yan, Z.; Ma, Z.; Xu, J.; Fayaz, M.; Zhou, C.; Wei, P.; Wang, P. Effect of Mineral Fertilizers on Microorganisms Community Characteristic during Leaf Litter Decomposition under Pinus Massoniana in a Subtropical Forest. *Appl. Soil Ecol.* **2024**, *199*, 105421. [CrossRef]
122. Bergmann, G.T.; Bates, S.T.; Eilers, K.G.; Lauber, C.L.; Caporaso, J.G.; Walters, W.A.; Knight, R.; Fierer, N. The Under-Recognized Dominance of Verrucomicrobia in Soil Bacterial Communities. *Soil Biol. Biochem.* **2011**, *43*, 1450–1455. [CrossRef] [PubMed]
123. Liu, B.; Hu, Y.; Wang, Y.; Xue, H.; Li, Z.; Li, M. Effects of Saline-Alkali Stress on Bacterial and Fungal Community Diversity in Leymus Chinensis Rhizosphere Soil. *Environ. Sci. Pollut. Res.* **2022**, *29*, 70000–70013. [CrossRef] [PubMed]
124. Li, K.; Lin, H.; Han, M.; Yang, L. Soil Metagenomics Reveals the Effect of Nitrogen on Soil Microbial Communities and Nitrogen-Cycle Functional Genes in the Rhizosphere of Panax Ginseng. *Front. Plant Sci.* **2024**, *15*, 1411073. [CrossRef]

125. Murphy, C.M.; Weller, D.L.; Bardsley, C.A.; Ingram, D.T.; Chen, Y.; Oryang, D.; Rideout, S.L.; Strawn, L.K. Survival of Twelve Pathogenic and Generic Escherichia Coli Strains in Agricultural Soils as Influenced by Strain, Soil Type, Irrigation Regimen, and Soil Amendment. *J. Food Prot.* **2024**, *87*, 100343. [CrossRef]
126. Wu, P.; Wang, J.; Guo, Z.; Cheng, Y.; Wu, J. Heavy Metals and Bacterial Community Determine Resistance Genes Distribution in Agricultural Soils Surrounding Long-Term Mining Area. *Appl. Soil Ecol.* **2024**, *202*, 105581. [CrossRef]
127. Buqori, D.M.A.I.; Sugiharto, B.; Suherman; Siswoyo, T.A.; Hariyono, K. Mitigating Drought Stress by Application of Drought-Tolerant *Bacillus* spp. Enhanced Root Architecture, Growth, Antioxidant and Photosynthetic Genes Expression in Sugarcane. *Sci. Rep.* **2025**, *15*, 5259. [CrossRef]
128. Wani, P.A.; Khan, M.S.; Zaidi, A. Chromium-Reducing and Plant Growth-Promoting Mesorhizobium Improves Chickpea Growth in Chromium-Amended Soil. *Biotechnol. Lett.* **2007**, *30*, 159–163. [CrossRef]
129. Umar, A.W.; Naeem, M.; Hussain, H.; Ahmad, N.; Xu, M. Starvation from within: How Heavy Metals Compete with Essential Nutrients, Disrupt Metabolism, and Impair Plant Growth. *Plant Sci.* **2025**, *353*, 112412. [CrossRef]
130. Gwóźdź, E.A.; Przymusiński, R.; Rucińska, R.; Deckert, J. Plant Cell Responses to Heavy Metals: Molecular and Physiological Aspects. *Acta Physiol. Plant.* **1997**, *19*, 459–465. [CrossRef]
131. Bhaduri, A.M.; Fulekar, M.H. Antioxidant Enzyme Responses of Plants to Heavy Metal Stress. *Rev. Environ. Sci. Biotechnol.* **2012**, *11*, 55–69. [CrossRef]
132. Dutta, S.; Mitra, M.; Agarwal, P.; Mahapatra, K.; De, S.; Sett, U.; Roy, S. Oxidative and Genotoxic Damages in Plants in Response to Heavy Metal Stress and Maintenance of Genome Stability. *Plant Signal. Behav.* **2018**, *13*, e1460048. [CrossRef] [PubMed]
133. Chu, D. Effects of Heavy Metals on Soil Microbial Community. *IOP Conf. Ser. Earth Environ. Sci.* **2018**, *113*, 012009. [CrossRef]
134. Drott, A. *Chemical Speciation and Transformation of Mercury in Contaminated Sediments*; Swedish University of Agricultural Sciences: Umeå, Sweden, 2009.
135. Xu, J.; Bravo, A.G.; Lagerkvist, A.; Bertilsson, S.; Sjöblom, R.; Kumpiene, J. Sources and Remediation Techniques for Mercury Contaminated Soil. *Environ. Int.* **2015**, *74*, 42–53. [CrossRef]
136. Ranjard, L.; Richaume, A.; Jocteur-Monrozier, L.; Nazaret, S. Response of Soil Bacteria to Hg (II) in Relation to Soil Characteristics and Cell Location. *FEMS Microbiol. Ecol.* **1997**, *24*, 321–331. [CrossRef]
137. Sarkar, S.; Pradeepa, N.; Balamurugan, A.; Ajay, D.; Premkumar, R. Effect of Heavy Metals (Pb, Hg, Fe and Cu) on Microflora of Tea Garden Soil. *Appl. Biol. Res.* **2009**, *11*, 12–16.
138. Nakatsu, C.H.; Carmosini, N.; Baldwin, B.; Beasley, F.; Kourtev, P.; Konopka, A. Soil Microbial Community Responses to Additions of Organic Carbon Substrates and Heavy Metals (Pb and Cr). *Appl. Environ. Microbiol.* **2005**, *71*, 7679–7689. [CrossRef]
139. Goswami, G.; Deka, P.; Das, P.; Bora, S.S.; Samanta, R.; Boro, R.C.; Barooah, M. Diversity and Functional Properties of Acid-Tolerant Bacteria Isolated from Tea Plantation Soil of Assam. *3 Biotech* **2017**, *7*, 229. [CrossRef]
140. Kostin, A.; Krechetov, P.; Chernitsova, O.; Terskaya, E. Geochemical Alterations of Forest Soils in Post-Mining Area (the Moscow Brown Coal Basin, Russia). In Proceedings of the EGU General Assembly Conference Abstracts, Online, 19–30 April 2021; p. EGU21-16057.
141. Illmer, P.; Marschall, K.; Schinner, F. Influence of Available Aluminium on Soil Micro-Organisms. *Lett. Appl. Microbiol.* **1995**, *21*, 393–397. [CrossRef]
142. Zhang, N.; Ma, Z.; Li, D.; Ni, H.; Sun, B.; Liang, Y. Soil pH Filters the Association Patterns of Aluminum-Tolerant Microorganisms in Rice Paddies. *mSystems* **2022**, *7*, e01022-21. [CrossRef]
143. Deng, B.; Gong, T.; Xu, C.; Zhang, X.; Cao, H.; Yuan, Q. The Potential of Black Soldier Fly Larvae Faeces and Sludge Residue as Fertilizer under Cu and Cd Stress. *J. Clean. Prod.* **2023**, *425*, 138981. [CrossRef]
144. Khoshru, B.; Mitra, D.; Nosratabad, A.F.; Reyhanitabar, A.; Mandal, L.; Farda, B.; Djebaili, R.; Pellegrini, M.; Guerra-Sierra, B.E.; Senapati, A. Enhancing Manganese Availability for Plants through Microbial Potential: A Sustainable Approach for Improving Soil Health and Food Security. *Bacteria* **2023**, *2*, 129–141. [CrossRef]
145. Faoro, H.; Alves, A.C.; Souza, E.M.; Rigo, L.U.; Cruz, L.M.; Al-Janabi, S.M.; Monteiro, R.A.; Baura, V.A.; Pedrosa, F.O. Influence of Soil Characteristics on the Diversity of Bacteria in the Southern Brazilian Atlantic Forest. *Appl. Environ. Microbiol.* **2010**, *76*, 4744–4749. [CrossRef] [PubMed]
146. He, Z.; Hu, Y.; Yin, Z.; Hu, Y.; Zhong, H. Microbial Diversity of Chromium-Contaminated Soils and Characterization of Six Chromium-Removing Bacteria. *Environ. Manag.* **2016**, *57*, 1319–1328. [CrossRef]
147. Wu, S.C.; Lu, C.-C. Evaluation of Applying an Alkaline Green Tea/Ferrous Iron System to Lindane Remediation Impacts to Soil and Plant Growth-Promoting Microbial Community. *Sci. Total Environ.* **2021**, *786*, 147511. [CrossRef]
148. Wu, S.C.; Luo, Y.M.; Cheung, K.C.; Wong, M.H. Influence of Bacteria on Pb and Zn Speciation, Mobility and Bioavailability in Soil: A Laboratory Study. *Environ. Pollut.* **2006**, *144*, 765–773. [CrossRef]
149. Nwuche, C.O.; Ugoji, E.O. Effects of Heavy Metal Pollution on the Soil Microbial Activity. *Int. J. Environ. Sci. Technol.* **2008**, *5*, 409–414. [CrossRef]

150. Mc Lean, E.O.; Watson, M.E. Soil Measurements of Plant-Available Potassium. In *ASA, CSSA, and SSSA Books*; Munson, R.D., Ed.; Wiley: Hoboken, NJ, USA, 1985; pp. 277–308.
151. Wu, J.; Peng, Z.; Guan, T.; Yang, H.; Tian, X. Diversity of Actinobacteria in Sediments of Qaidam Lake and Qinghai Lake, China. *Arch. Microbiol.* **2021**, *203*, 2875–2885. [CrossRef]
152. Landeweert, R.; Hoffland, E.; Finlay, R.D.; Kuyper, T.W.; van Breemen, N. Linking Plants to Rocks: Ectomycorrhizal Fungi Mobilize Nutrients from Minerals. *Trends Ecol. Evol.* **2001**, *16*, 248–254. [CrossRef]
153. Calvaruso, C.; Turpault, M.-P.; Frey-Klett, P. Root-Associated Bacteria Contribute to Mineral Weathering and to Mineral Nutrition in Trees: A Budgeting Analysis. *Appl. Environ. Microbiol.* **2006**, *72*, 1258–1266. [CrossRef]
154. Lei, M.; Wang, Y.; Guo, G.; Zhang, D.; Zhao, X. The Bio-Availability and Accumulation of the Trace Elements in Rock-Soil-Fruit System in Carbonatite Regions of Different Stratums: Critical Soil Factors and Transfer Models. *Sci. Total Environ.* **2021**, *760*, 143328. [CrossRef] [PubMed]
155. Gómez-Armesto, A.; Méndez-López, M.; Pontevedra-Pombal, X.; García-Rodeja, E.; Alonso-Vega, F.; Arias-Estévez, M.; Nóvoa-Muñoz, J.C. Soil Properties Influencing Hg Vertical Pattern in Temperate Forest Podzols. *Environ. Res.* **2021**, *193*, 110552. [CrossRef] [PubMed]
156. Deng, J.; Yu, J.; Wang, X.; Yu, D.; Ma, H.; Wu, Y.; Yu, C.; Pu, S. Spatial Distribution and Migration Characteristics of Heavy Metals at an Abandoned Industrial Site in the Southwest of China. *J. Hazard. Mater.* **2024**, *480*, 136447. [CrossRef] [PubMed]
157. Matsuura, H.; Hokura, A.; Katsuki, F.; Itoh, A.; Haraguchi, H. Multielement Determination and Speciation of Major-to-Trace Elements in Black Tea Leaves by ICP-AES and ICP-MS with the Aid of Size Exclusion Chromatography. *Anal. Sci.* **2001**, *17*, 391–398. [CrossRef]
158. Pal, A.; Wauters, G.; Paul, A.K. Nickel Tolerance and Accumulation by Bacteria from Rhizosphere of Nickel Hyperaccumulators in Serpentine Soil Ecosystem of Andaman, India. *Plant Soil* **2007**, *293*, 37–48. [CrossRef]
159. Xia, X.; Ji, J.; Yang, Z.; Han, H.; Huang, C.; Li, Y.; Zhang, W. Cadmium Risk in the Soil-Plant System Caused by Weathering of Carbonate Bedrock. *Chemosphere* **2020**, *254*, 126799. [CrossRef]
160. Li, X.; Teng, L.; Fu, T.; He, T.; Wu, P. Comparing the Effects of Calcium and Magnesium Ions on Accumulation and Translocation of Cadmium in Rice. *Environ. Sci. Pollut. Res.* **2022**, *29*, 41628–41639. [CrossRef]
161. Osvalde, A.; Karlsons, A.; Cekstere, G.; Āboliņa, L. Leaf Nutrient Status of Commercially Grown Strawberries in Latvia, 2014–2022: A Possible Yield-Limiting Factor. *Plants* **2023**, *12*, 945. [CrossRef]
162. Kou, B.; Yuan, Y.; Zhu, X.; Ke, Y.; Wang, H.; Yu, T.; Tan, W. Effect of Soil Organic Matter-Mediated Electron Transfer on Heavy Metal Remediation: Current Status and Perspectives. *Sci. Total Environ.* **2024**, *917*, 170451. [CrossRef]
163. Zhu, B.-L.; Qi, C.-L.; Zhang, Y.-H.; Bisson, T.; Xu, Z.; Fan, Y.-J.; Sun, Z.-X. Synthesis, Characterization and Acid-Base Properties of Kaolinite and Metal (Fe, Mn, Co) Doped Kaolinite. *Appl. Clay Sci.* **2019**, *179*, 105138. [CrossRef]
164. Cao, H.; Liu, X.; Feng, B.; Sun, J.; Ma, D.; Chen, X.; Li, H. Effect of pH on the Surface Charges of Permanently/Variably Charged Soils and Clay Minerals. *Sci. Rep.* **2024**, *14*, 23169. [CrossRef] [PubMed]
165. Liu, G.; Hanlon, E. Soil pH Range for Optimum Commercial Vegetable Production: HS1207/HS1207, 10/2012. *Edis* **2012**, *2012*. [CrossRef]
166. Khoury, H.N.; Al-Zoubi, A.S. Origin and Characteristics of Cr-Smectite from Suweileh Area, Jordan. *Appl. Clay Sci.* **2014**, *90*, 43–52. [CrossRef]
167. Proust, D. Sorption and Distribution of Zn in a Sludge-Amended Soil: Influence of the Soil Clay Mineralogy. *J. Soils Sediments* **2015**, *15*, 607–622. [CrossRef]
168. Massonne, H.-J.; Schreyer, W. Phengite Geobarometry Based on the Limiting Assemblage with K-Feldspar, Phlogopite, and Quartz. *Contrib. Mineral. Petrol.* **1987**, *96*, 212–224. [CrossRef]
169. Zi, L.; Xingkai, H.; Hongling, X.; Bin, Z.; Qingsong, P.; Chensheng, W.; Heng, W.; Hua, J. Migration Characteristics of Elements in the Rock-Soil System and Suitability Evaluation of Orange Planting in Yaqueling Area, Yichang, Hubei Province. *Geol. China* **2020**, *47*, 1853–1868.
170. Furtak, K.; Grządziel, J.; Gałązka, A.; Niedźwiecki, J. Analysis of Soil Properties, Bacterial Community Composition, and Metabolic Diversity in Fluvisols of a Floodplain Area. *Sustainability* **2019**, *11*, 3929. [CrossRef]
171. Wang, C.Y.; Li, X.F.; Xiao, R.; Bai, Y.P.; Yang, F.; Mao, W.; Jiang, S.K. Elements Mobilization of Mineralized Porphyry Rocks during Hydrothermal Alteration at Zhushahong Porphyry Copper Deposit, Dexing District, South China. *Acta Petrol. Sin.* **2012**, *28*, 3869–3886.
172. Olagoke, F.K.; Bettermann, A.; Nguyen, P.T.B.; Redmile-Gordon, M.; Babin, D.; Smalla, K.; Nesme, J.; Sørensen, S.J.; Kalbitz, K.; Vogel, C. Importance of Substrate Quality and Clay Content on Microbial Extracellular Polymeric Substances Production and Aggregate Stability in Soils. *Biol. Fertil. Soils* **2022**, *58*, 435–457. [CrossRef]
173. Sazykin, I.; Khmelevtsova, L.; Azhogina, T.; Sazykina, M. Heavy Metals Influence on the Bacterial Community of Soils: A Review. *Agriculture* **2023**, *13*, 653. [CrossRef]

174. Zhang, M.; Wu, Y.; Qu, C.; Huang, Q.; Cai, P. Microbial Extracellular Polymeric Substances (EPS) in Soil: From Interfacial Behaviour to Ecological Multifunctionality. *Geo-Bio Interfaces* **2024**, *1*, e4. [CrossRef]
175. Boedeker, C.; Schüler, M.; Reintjes, G.; Jeske, O.; van Teeseling, M.C.; Jogler, M.; Rast, P.; Borchert, D.; Devos, D.P.; Kucklick, M. Determining the Bacterial Cell Biology of Planctomycetes. *Nat. Commun.* **2017**, *8*, 14853. [CrossRef] [PubMed]
176. Helios-Rybicka, E.; Wójcik, R. Competitive Sorption/Desorption of Zn, Cd, Pb, Ni, Cu, and Cr by Clay-Bearing Mining Wastes. *Appl. Clay Sci.* **2012**, *65*, 6–13. [CrossRef]
177. Spence, A.; Kelleher, B.P. FT-IR Spectroscopic Analysis of Kaolinite–Microbial Interactions. *Vib. Spectrosc.* **2012**, *61*, 151–155. [CrossRef]
178. Sauro, F.; Cappelletti, M.; Ghezzi, D.; Columbu, A.; Hong, P.-Y.; Zowawi, H.M.; Carbone, C.; Piccini, L.; Vergara, F.; Zannoni, D. Microbial Diversity and Biosignatures of Amorphous Silica Deposits in Orthoquartzite Caves. *Sci. Rep.* **2018**, *8*, 17569. [CrossRef]
179. Ghezzi, D.; Salvi, L.; Costantini, P.E.; Firrincieli, A.; Iorio, M.; Lopo, E.; Sosio, M.; Elbanna, A.H.; Khalil, Z.G.; Capon, R.J. Ancient and Remote Quartzite Caves as a Novel Source of Culturable Microbes with Biotechnological Potential. *Microbiol. Res.* **2024**, *286*, 127793. [CrossRef]
180. Wu, B.; Luo, H.; Wang, X.; Liu, H.; Peng, H.; Sheng, M.; Xu, F.; Xu, H. Effects of Environmental Factors on Soil Bacterial Community Structure and Diversity in Different Contaminated Districts of Southwest China Mine Tailings. *Sci. Total Environ.* **2022**, *802*, 149899. [CrossRef]
181. Sun, F.; Xu, Z.; Fan, L. Response of Heavy Metal and Antibiotic Resistance Genes and Related Microorganisms to Different Heavy Metals in Activated Sludge. *J. Environ. Manag.* **2021**, *300*, 113754. [CrossRef]
182. Ge, L.; Yuan, X.; Zhang, L.; Li, H.; Liu, X.; Zhu, X. Uncovering the Relationship Between Soil Bacterial Community and Heavy Metals in a Copper Waste Pile. *Minerals* **2024**, *14*, 1237. [CrossRef]
183. Mundra, S.; Pundir, M.; Lothenbach, B.; Kammer, D.S.; Angst, U.M. Navigating the Complexities of Multiple Redox State Interactions in Aqueous Systems. *arXiv* **2025**, arXiv:2501.11536. [CrossRef]
184. Ouimet, R.; Duchesne, L. Base Cation Mineral Weathering and Total Release Rates from Soils in Three Calibrated Forest Watersheds on the Canadian Boreal Shield. *Can. J. Soil Sci.* **2005**, *85*, 245–260. [CrossRef]
185. Zeng, Q.; Dong, Y.; An, S. Bacterial Community Responses to Soils along a Latitudinal and Vegetation Gradient on the Loess Plateau, China. *PLoS ONE* **2016**, *11*, e0152894. [CrossRef] [PubMed]
186. Aallam, Y.; Maliki, B.E.; Dhiba, D.; Lemriss, S.; Souiri, A.; Haddioui, A.; Tarkka, M.; Hamdali, H. Multiple Potential Plant Growth Promotion Activities of Endemic Streptomyces Spp. from Moroccan Sugar Beet Fields with Their Inhibitory Activities against *Fusarium* spp. *Microorganisms* **2021**, *9*, 1429. [CrossRef] [PubMed]
187. Ribeiro, P.G.; Souza, J.M.P.; Rodrigues, M.; Ribeiro, I.C.A.; de Carvalho, T.S.; Lopes, G.; Li, Y.C.; Guilherme, L.R.G. Hydrothermally-Altered Feldspar as an Environmentally-Friendly Technology to Promote Heavy Metals Immobilization: Batch Studies and Application in Smelting-Affected Soils. *J. Environ. Manag.* **2021**, *291*, 112711. [CrossRef]
188. Wang, P.; Shen, X.; Qiu, S.; Zhang, L.; Ma, Y.; Liang, J. Clay-Based Materials for Heavy Metals Adsorption: Mechanisms, Advancements, and Future Prospects in Environmental Remediation. *Crystals* **2024**, *14*, 1046. [CrossRef]
189. Welch, S.A.; Barker, W.W.; Banfield, J.F. Microbial Extracellular Polysaccharides and Plagioclase Dissolution. *Geochim. Cosmochim. Acta* **1999**, *63*, 1405–1419. [CrossRef]
190. Ortiz-Castillo, J.E.; Mirazimi, M.; Mohammadi, M.; Dy, E.; Liu, W. The Role of Microorganisms in the Formation, Dissolution, and Transformation of Secondary Minerals in Mine Rock and Drainage: A Review. *Minerals* **2021**, *11*, 1349. [CrossRef]
191. Han, X.; Pan, Y. Mineralization Products of Iron-Reducing Bacteria and Their Implications to Iron Formations Deposition. *Acta Petrol. Sin.* **2024**, *40*, 1299–1310. [CrossRef]
192. Puente-Sánchez, F.; Macías-Pérez, L.A.; Campbell, K.L.; Royo-Llonch, M.; Balagué, V.; Sánchez, P.; Tamames, J.; Mundy, C.J.; Pedrós-Alió, C. Bacterioplankton Taxa Compete for Iron along the Early Spring–Summer Transition in the Arctic Ocean. *Ecol. Evol.* **2024**, *14*, e11546. [CrossRef]
193. Jaisi, D.P.; Eberl, D.D.; Dong, H.; Kim, J. The Formation of Illite from Nontronite by Mesophilic and Thermophilic Bacterial Reaction. *Clays Clay Miner.* **2011**, *59*, 21–33. [CrossRef]
194. Yang, H.; Hu, Z.; Xiao, R.; Liu, Z.; Zhang, M.; Li, Y.-L.; Wu, S.; Fu, Z. Identification and Performance of Endophytic Actinobacteria Ahn65 with Functions of Growth Promotion and Disease Resistance for Rice. *Physiol. Mol. Plant Pathol.* **2024**, *134*, 102418. [CrossRef]
195. Choi, J.-S.; Seok, Y.-J.; Cho, Y.-H.; Roe, J.-H. Iron-Induced Respiration Promotes Antibiotic Resistance in Actinomycete Bacteria. *mBio* **2022**, *13*, e00425-22. [CrossRef] [PubMed]
196. Kuffner, M.; De Maria, S.; Puschenreiter, M.; Fallmann, K.; Wieshammer, G.; Gorfer, M.; Strauss, J.; Rivelli, A.R.; Sessitsch, A. Culturable Bacteria from Zn-and Cd-Accumulating Salix Caprea with Differential Effects on Plant Growth and Heavy Metal Availability. *J. Appl. Microbiol.* **2010**, *108*, 1471–1484. [CrossRef] [PubMed]

197. Dangar, K.; Ramani, K.; Changela, D. Analyzing the Capabilities of Actinobacteria for Remediation Through Metagenomic Analysis of Contaminated Habitats. In *Microbial BioTechnology for Sustainable Agriculture Volume 1*; Arora, N.K., Bouizgarne, B., Eds.; Microorganisms for Sustainability; Springer Nature: Singapore, 2022; Volume 33, pp. 471–487.
198. Li, Y.; Shi, X.; Chen, Y.; Luo, S.; Qin, Z.; Chen, S.; Wu, Y.; Yu, F. Quantitative Proteomic Analysis of the Mechanism of Cd Toxicity in Enterobacter Sp. FM-1: Comparison of Different Growth Stages. *Environ. Pollut.* **2023**, *336*, 122513. [CrossRef]
199. Niu, S.; Song, H.; Zhang, X.; Bao, X.; Li, T.; He, L.; Li, Y.; Li, Y.; Zhang, D.; Bai, J. The Cd Resistant Mechanism of Proteus Mirabilis Ch8 through Immobilizing and Detoxifying. *Ecotoxicol. Environ. Saf.* **2024**, *278*, 116432. [CrossRef]
200. Veluchamy, C.; Sharma, A.; Thiagarajan, K. Assessing the Impact of Heavy Metals on Bacterial Diversity in Coastal Regions of Southeastern India. *Environ. Monit. Assess.* **2024**, *196*, 828. [CrossRef]
201. Zhang, J.; Shi, Q.; Fan, S.; Zhang, Y.; Zhang, M.; Zhang, J. Distinction between Cr and Other Heavy–Metal–Resistant Bacteria Involved in C/N Cycling in Contaminated Soils of Copper Producing Sites. *J. Hazard. Mater.* **2021**, *402*, 123454. [CrossRef]
202. Liu, Q.; Cui, H.; Yang, W.; Wang, F.; Liao, H.; Zhu, Q.; Qin, S.; Lu, P. Soil Conditioner Improves Soil Properties, Regulates Microbial Communities, and Increases Yield and Quality of Uncaria Rhynchophylla. *Sci. Rep.* **2024**, *14*, 13398. [CrossRef]
203. Li, X.; Sun, M.; Zhang, L.; Finlay, R.D.; Liu, R.; Lian, B. Widespread Bacterial Responses and Their Mechanism of Bacterial Metallogenic Detoxification under High Concentrations of Heavy Metals. *Ecotoxicol. Environ. Saf.* **2022**, *246*, 114193. [CrossRef]
204. Nnaji, N.D.; Anyanwu, C.U.; Miri, T.; Onyeaka, H. Mechanisms of Heavy Metal Tolerance in Bacteria: A Review. *Sustainability* **2024**, *16*, 11124. [CrossRef]
205. Zhu, Y.; Wang, L.; Ma, J.; Hua, Z.; Chen, F. Metal-Tolerant Microbial Succession Mediated by Mining Reclamation Improves Network Stress Resistance. *Water. Air. Soil Pollut.* **2024**, *235*, 736. [CrossRef]
206. Zhang, F.; Xie, Y.; Peng, R.; Ji, X.; Bai, L. Heavy Metals and Nutrients Mediate the Distribution of Soil Microbial Community in a Typical Contaminated Farmland of South China. *Sci. Total Environ.* **2024**, *947*, 174322. [CrossRef] [PubMed]
207. Gao, X.; Zhang, S.; Zhao, X.; Long, H. Evaluation of Potassium Application on Tomato Performance and Rhizosphere Bacterial Communities under Negative Pressure Irrigation of Greenhouse-Grown. *J. Plant Nutr.* **2020**, *43*, 317–326. [CrossRef]
208. Xu, Q.; Fu, H.; Zhu, B.; Hussain, H.A.; Zhang, K.; Tian, X.; Duan, M.; Xie, X.; Wang, L. Potassium Improves Drought Stress Tolerance in Plants by Affecting Root Morphology, Root Exudates, and Microbial Diversity. *Metabolites* **2021**, *11*, 131. [CrossRef]
209. Zhang, H.; Li, C.; Zhang, L.; Zhang, Q. Effects of Potassium on Tea Quality Are Associated with the Accumulation of Anthocyanins in Tea Plant. *Hortic. Environ. Biotechnol.* **2025**, *66*, 287–296. [CrossRef]
210. Ghosh, S.; Das, A.P. Metagenomic Insights into the Microbial Diversity in Manganese-Contaminated Mine Tailings and Their Role in Biogeochemical Cycling of Manganese. *Sci. Rep.* **2018**, *8*, 8257. [CrossRef]
211. Gunduz, M.; Al-Ajji, I. Employment of CHAID and CRT Decision Tree Algorithms to Develop Bid/No-Bid Decision-Making Models for Contractors. *Eng. Constr. Archit. Manag.* **2022**, *29*, 3712–3736. [CrossRef]
212. Liu, Y.; Zhang, D.; Lu, G. Region-Based Image Retrieval with High-Level Semantics Using Decision Tree Learning. *Pattern Recognit.* **2008**, *41*, 2554–2570. [CrossRef]
213. Gupta, B.; Rawat, A.; Jain, A.; Arora, A.; Dhami, N. Analysis of Various Decision Tree Algorithms for Classification in Data Mining. *Int. J. Comput. Appl.* **2017**, *163*, 15–19. [CrossRef]
214. Chen, X.; Ren, Y.; Li, C.; Shang, Y.; Ji, R.; Yao, D.; He, Y. Study on Factors Influencing the Migration of Heavy Metals from Soil to Vegetables in a Heavy Industry City. *Sustainability* **2024**, *16*, 11084. [CrossRef]
215. Gong, Y.; Ren, W.; Li, F.; Jiang, Y.; Zhang, Z. The Role of Soil Elemental Forms in the Soil-Plant Migration System: An Example of Heavy Metals in Epimedium Production Areas. *Environ. Technol. Innov.* **2024**, *36*, 103800. [CrossRef]
216. Yang, Y.; Liu, J.; Zhu, R.; Chen, Q.; Wei, H.; Chen, M.; Xian, H.; He, H. Surface-Induced Oxidation of Mn (II) and Crystallization of Manganese (Hydr) Oxides on Clay Minerals. *Geochim. Cosmochim. Acta* **2023**, *363*, 129–146. [CrossRef]
217. Zulfiqar, U.; Haider, F.U.; Maqsood, M.F.; Mohy-Ud-Din, W.; Shabaan, M.; Ahmad, M.; Kaleem, M.; Ishfaq, M.; Aslam, Z.; Shahzad, B. Recent Advances in Microbial-Assisted Remediation of Cadmium-Contaminated Soil. *Plants* **2023**, *12*, 3147. [CrossRef]
218. Tian, L.; Wang, D.; Liu, Y.; Wei, M.; Han, X.; Sun, X.; Yin, L.; Luo, G. Construction of Genetically Engineered Escherichia Coli Cell Factory for Enhanced Cadmium Bioaccumulation in Wastewater. *Water* **2024**, *16*, 1759. [CrossRef]
219. Feng, F.; Lan, B.; He, W.; Wen, X.; Chen, S.; Tu, C. Biogenic Mn Oxide Generation and Mn(II) Removal by a Manganese Oxidizing Bacterium Bacillus Sp. Strain M2. *Appl. Biochem. Biotechnol.* **2024**, *196*, 8366–8380. [CrossRef]
220. Xu, H.; He, E.; Peijnenburg, W.J.; Song, L.; Zhao, L.; Xu, X.; Cao, X.; Qiu, H. Contribution of Pristine and Reduced Microbial Extracellular Polymeric Substances of Different Sources to Cu (II) Reduction. *J. Hazard. Mater.* **2021**, *415*, 125616. [CrossRef]
221. Fan, L.; Sun, F.; Yang, Z. Metagenomic Analyses Reveal Nitrogen Metabolism Responses to Copper and Chromium Contamination in Sludge-Based Microbial Communities. *J. Water Process Eng.* **2022**, *49*, 102951. [CrossRef]
222. Du, J.; Yuan, Y.; Li, J.; Zhang, S.; Ren, Y. Preliminary Study on Mercury Pollution Affecting Soil Bacteria near a Mercury Mining Area. *Front. Microbiol.* **2025**, *16*, 1539059. [CrossRef]

223. Meng, W.; Lv, Z.; Feng, M.; Zhang, S.; Mai, F. The Origin of Authigenic Illite in Tight Sandstones and Its Effect on the Formation of Relatively High-Quality Reservoirs: A Case Study on Sandstones in the 4th Member of Xujiahe Formation, Western Sichuan Basin. *Acta Pet. Sin.* **2011**, *32*, 783–790.
224. Li, J.-L.; Wang, X.-S.; Wang, Z.; Huang, J.; Gao, J. Ca–Zn Isotope Fractionation during Fluid–Rock Interaction in Subduction Zones and Its Implication for Deep Carbon Cycle. *Chem. Geol.* **2024**, *670*, 122425. [CrossRef]
225. Kaboré, O.D.; Godreuil, S.; Drancourt, M. Planctomycetes as Host-Associated Bacteria: A Perspective That Holds Promise for Their Future Isolations, by Mimicking Their Native Environmental Niches in Clinical Microbiology Laboratories. *Front. Cell. Infect. Microbiol.* **2020**, *10*, 519301. [CrossRef]
226. Wu, G.; Huang, A.; Wen, Y.; Wang, H.; Wang, J.; Luo, F.; Wu, M. Euendolithic Cyanobacteria and Proteobacteria Together Contribute to Trigger Bioerosion in Aquatic Environments. *Front. Microbiol.* **2022**, *13*, 938359. [CrossRef]
227. Kong, F.; Lu, S. Inorganic Amendments Improve Acidic Paddy Soils: Effects on Soil Properties, Al Fractions, and Microbial Communities. *Chemosphere* **2023**, *331*, 138758. [CrossRef]
228. Shabtai, I.A.; Wilhelm, R.C.; Schweizer, S.A.; Höschen, C.; Buckley, D.H.; Lehmann, J. Calcium Promotes Persistent Soil Organic Matter by Altering Microbial Transformation of Plant Litter. *Nat. Commun.* **2023**, *14*, 6609. [CrossRef]
229. Jing, T.; Li, J.; He, Y.; Shankar, A.; Saxena, A.; Tiwari, A.; Maturi, K.C.; Solanki, M.K.; Singh, V.; Eissa, M.A. Role of Calcium Nutrition in Plant Physiology: Advances in Research and Insights into Acidic Soil Conditions-A Comprehensive Review. *Plant Physiol. Biochem.* **2024**, *210*, 108602. [CrossRef]